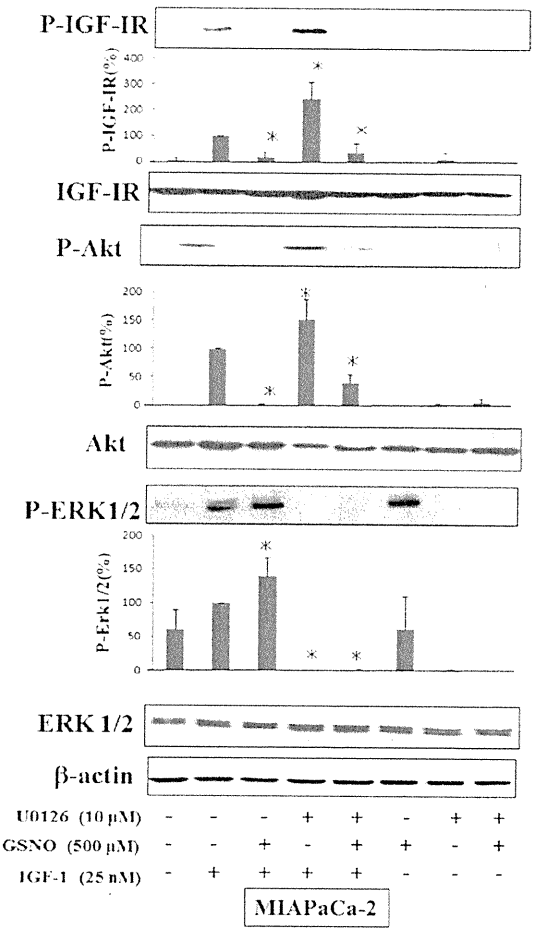

Figure 1. Regulation of insulin-like growth factor (IGF) signaling by nitric oxide (NO) donor and MEK inhibitor in MIAPaCa-2 cells. MIAPaCa-2 cells were incubated in DMEM with 10% FBS overnight and grown to 80% confluency. The cells were then incubated with S-nitrosoglutathione (GSNO) (500 μM) and U0126 (10 μM) for 6 h. After the starvation of serum for 2 h, the cells were incubated with IGF-I (25 nM) for 5 min and then harvested. Cell lysates were subjected to immunoblotting (IB). All experiments were repeated three times and similar results were obtained. Bands of interest were scanned by using Colorio GT-X970 and were quantified by using NIH Image 1.62 software. The results of densitrometry analysis of each band were compared to control, which was the band of IGF-I-stimulated p-Akt, p-ERK1/2, and p-IGF-IR without the administration of either GSNO or U0126. Error bars indicate the standard errors of the means. *P<0.05 compared to control.

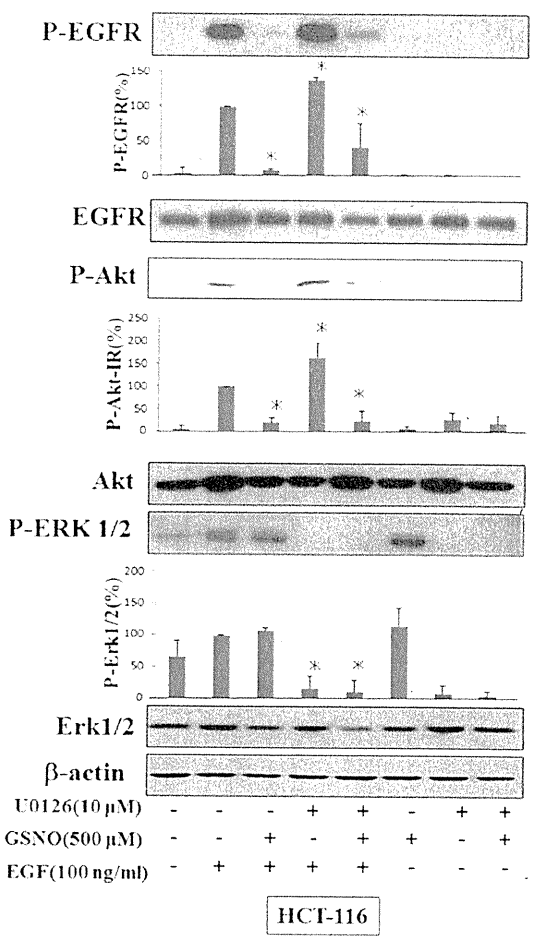

Figure 2. Regulation of EGF signaling by NO donor and MEK inhibitor in HCT-116 cells. HCT-116 cells were incubated in RPMI-1640 with 10% FBS overnight and grown to 80% confluency. The cells were then incubated with GSNO (500 μM) and U0126 (10 μM) for 6 h. After the starvation of serum for 2 h, the cells were incubated with EGF (100 ng/ml) for 5 min and then harvested. Cell lysates were subjected to immunoblotting. All experiments were repeated three times and similar results were obtained. Bands of interest were scanned by using Colorio GT-X970 and were quantified with NIH Image 1.62 software. The results of densitrometry analysis of each band were compared to control, which was the band of EGF-stimulated p-Akt, p-ERK1/2, and p-IGF-IR without the administration of either GSNO or U0126. Error bars indicate the standard errors of the means. *P<0.05, compared to control.

NO donor and MEK inhibitor influence EGF signaling in HCT-116 cells. Stimulation of EGF resulted in marked tyrosine phosphorylation of EGFR, Akt and ERK1/2 in HCT-116 cells. GSNO inhibited EGF-stimulated phosphorylation of EGFR and Akt. However, GSNO induced phosphorylation of ERK1/2 without stimulation of EGF, and enhanced EGF-stimulated phosphorylation of ERK1/2. U0126 inhibited EGF-stimulated phosphorylation of ERK1/2. On the other hand, surprisingly, U0126 enhanced EGF-stimulated tyrosine phosphorylation of EGFR without the influence of EGFR protein expression. In addition, U0126 upregulates EGF-stimulated phosphorylation of Akt. The combination of GSNO and U0126 inhibited EGF-stimulated phosphorylation of EGFR, Akt and ERK1/2 without the influence of EGFR, Akt, and ERK1/2 protein expression (Fig. 2).

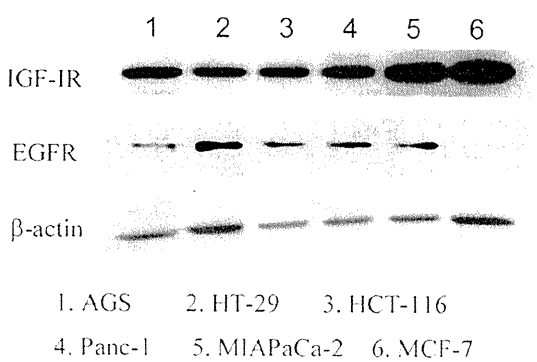

Figure 3. IGF-IR and EGFR protein expression in cancer cells. Cell lysates of MIAPaCa-2 cells, HCT-116, Panc-1, MCF-7, HT-29 and AGS cells were subjected to immunoblotting and then IGF-IR and EGFR protein was detected.

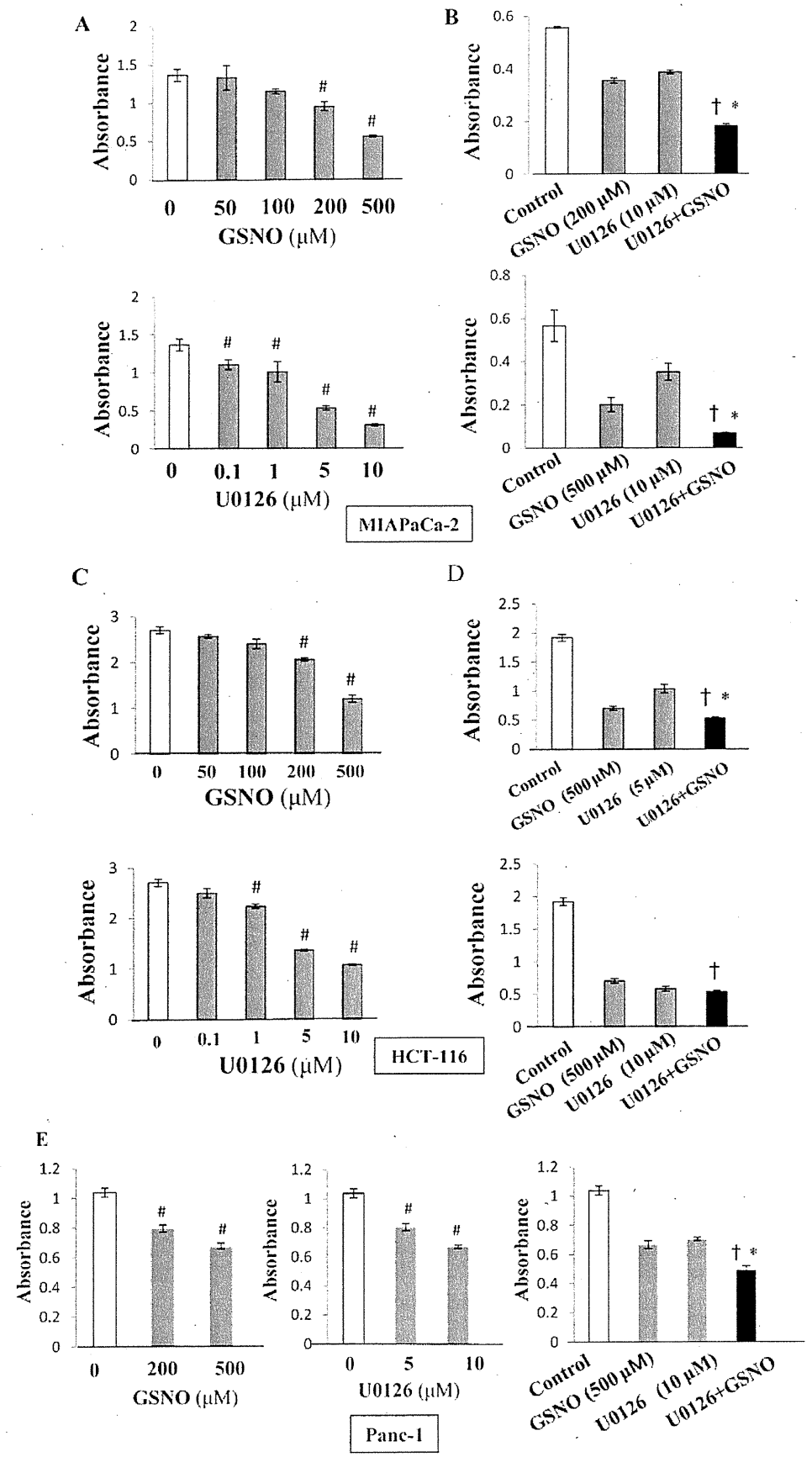

Figure 4. NO donor alone and MEK inhibitor alone significantly inhibit the proliferation of cancer cells in a dose-dependent manner, when the cells were incubated in medium containing with FBS. The combination of NO donor and MEK inhibitor inhibit the proliferation of MIAPaCa-2 cells compared to either NO donor or MEK inhibitor alone.

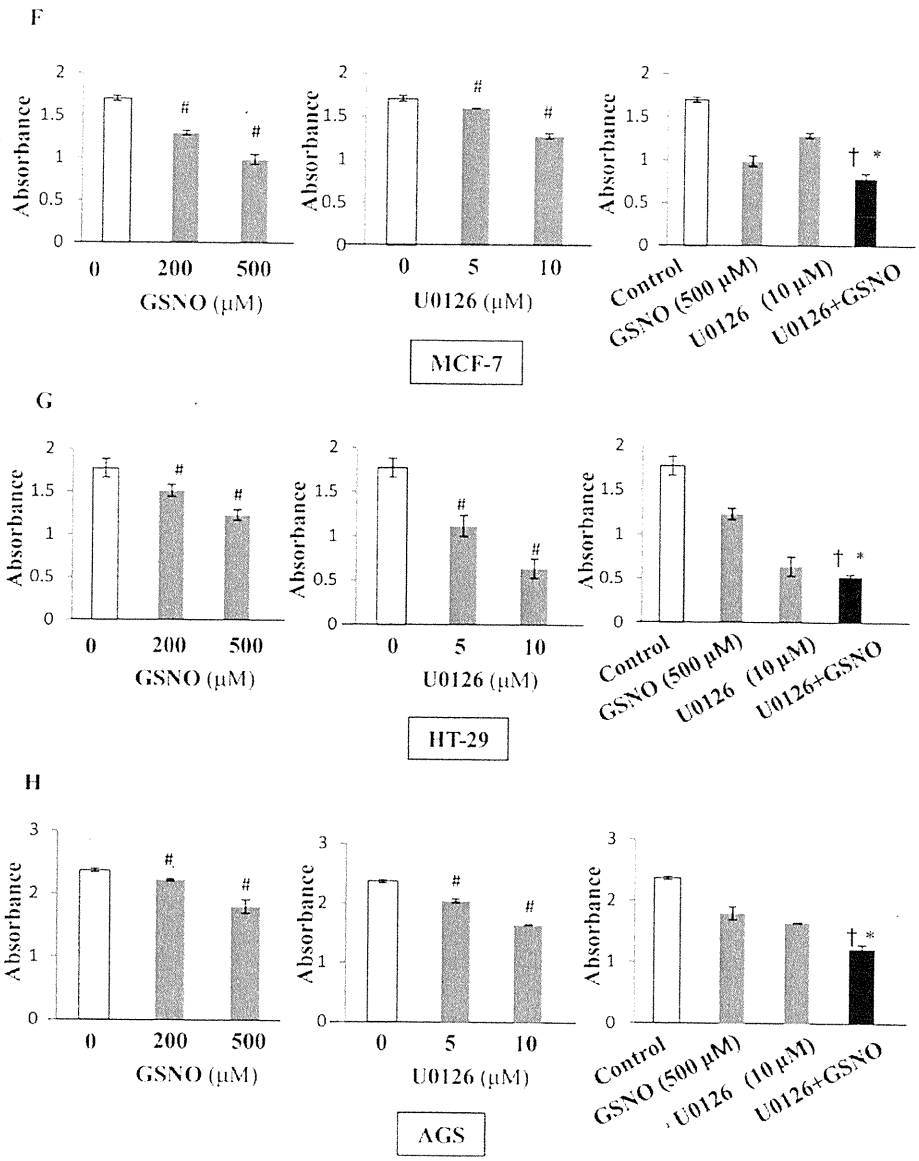

Figure 4. Continued. MIAPaCa-2, HCT-116, Panc-1, MCF-7, HT-29 and AGS cells were incubated with GSNO (0-500 μM) alone or U0126 (0-10 μM) alone in medium containing 10% FBS for 72 h. Cancer cells, were incubated with the combination of GSNO and U0126 in medium containing 10% FBS for 72 h and then cell proliferation was determined. (A and B) MIAPaCa-2 cells, (C and D) HCT-116 cells, (E) Panc-1 cells, (F) MCF-7 cells, (G) HT-29 cells, (H) AGS cells. #P<0.05, compared to control; †P<0.05, compared to GSNO alone; *P<0.05, compared to U0126 alone.

The combination of NO donor and MEK inhibitor inhibits the proliferation of cancer cell lines compared to either NO donor or MEK inhibitor alone. IGF-IR protein was expressed in MIAPaCa-2, HCT-116, Panc-1, MCF-7, HT-29 and AGS cells, and EGFR protein was expressed in MIAPaCa-2, HCT-116, Panc-1, HT-29 and AGS cells (Fig. 3). To evaluate the effects of the combination of NO donor and MEK inhibitor on MIAPaCa-2, HCT-116, Panc-1, MCF-7, HT-29 and AGS cells, we analyzed cell proliferation using an MTT assay after the cells were treated with NO donor and MEK inhibitor for 72 h. As shown in Fig. 4A, GSNO alone and MEK inhibitor alone significantly inhibited the proliferation of MIAPaCa-2 cells in a dose-dependent manner when the cells were incubated with FBS. The combination of NO donor (200 μM, 500 μM) and MEK inhibitor (10 μM) decreased the proliferation of MIAPaCa-2 cells compared to either NO donor or MEK inhibitor alone when the cells were incubated with FBS (Fig. 4B). Similar results were found in HCT-116, Panc-1, MCF-7, HT-29 and AGS cells (Fig. 4C-H).

GSNO alone and MEK inhibitor alone significantly inhibited the proliferation of MIAPaCa-2 cells in a dose-dependent manner when the cells were incubated with IGF-I (Fig. 5A and B). The combination of NO donor (100 μM) and MEK inhibitor (10 μM) decreased the proliferation of MIAPaCa-2 cells compared to either NO donor or MEK inhibitor alone when the cells were incubated with IGF-I (Fig. 5C).

GSNO alone and MEK inhibitor alone significantly inhibited the proliferation of HCT-116 cells in a dose-dependent manner when the cells were incubated with EGF

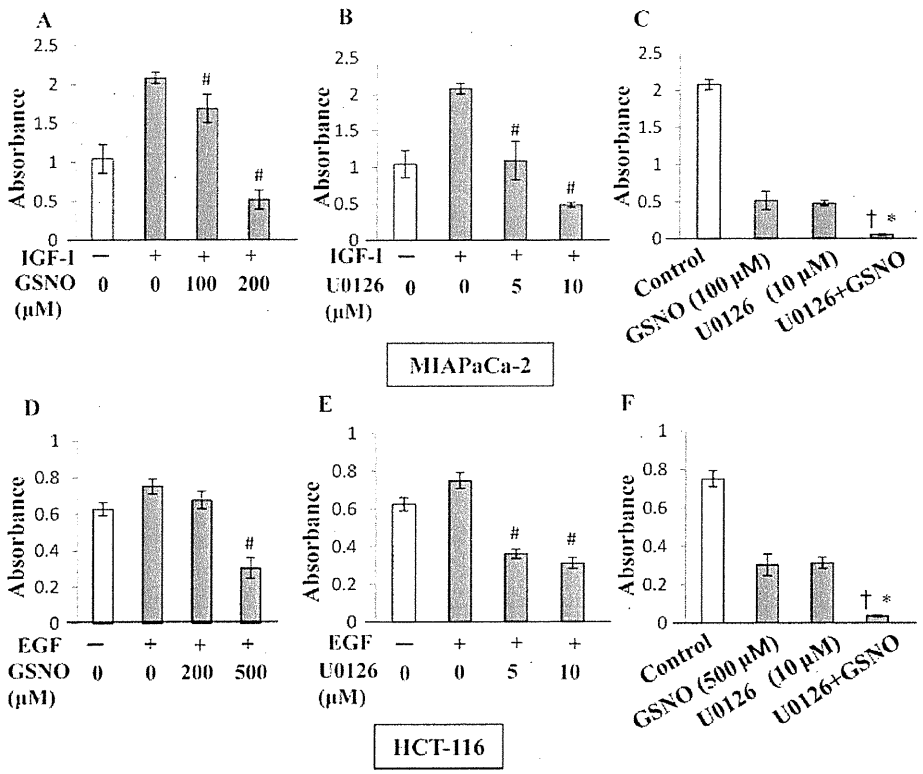

Figure 5. NO donor alone and MEK inhibitor alone significantly inhibit the proliferation of MIAPaCa-2 cells in a dose-dependent manner, when the cells were incubated with IGF-I (A and B). The combination of NO donor and MEK inhibitor inhibits the proliferation of MIAPaCa-2 cells compared to either NO donor or MEK inhibitor alone (C). MIAPaCa-2 cells were incubated with the combination of GSNO and U0126 in medium containing IGF-I (100 nM) for 72 h and then cell proliferation was determined. #P<0.05, compared to control; †P< 0.01, compared to GSNO alone; *P<0.01, compared to U0126 alone. NO donor alone and MEK inhibitor alone significantly inhibit the proliferation of HCT-116 cells in a dose-dependent manner, when the cells were incubated with EGF (D and E). The combination of NO donor and MEK inhibitor inhibits the proliferation of HCT-116 cells compared to either NO donor or MEK inhibitor alone (F). HCT-116 cells were incubated with the combination of GSNO and U0126 in medium containing EGF (100 ng/ml) for 72 h and then cell proliferation was determined. #P<0.05, compared to control; †P<0.01, compared to GSNO alone; *P<0.01, compared to U0126 alone.

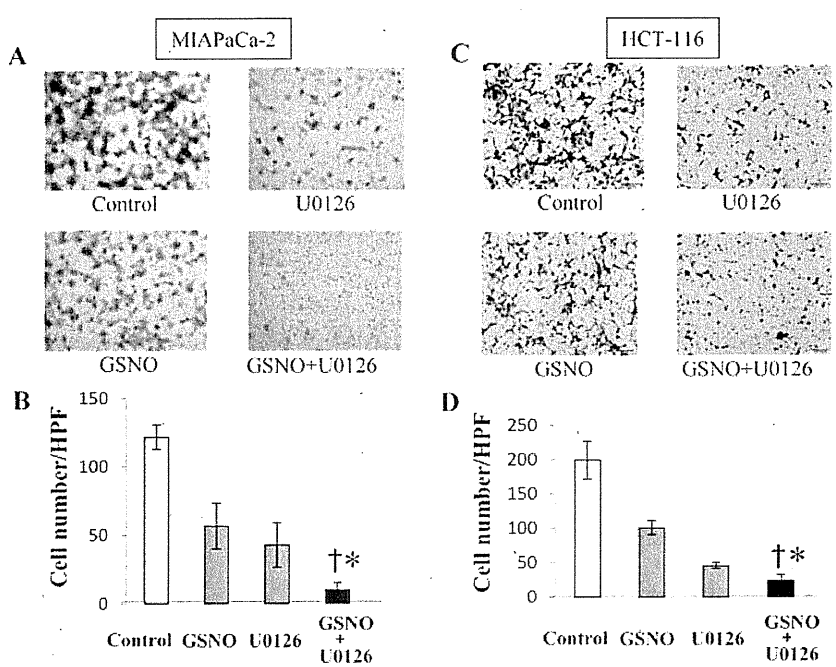

Figure 6. The combination of NO donor and MEK inhibitor inhibits the invasion of MIAPaCa-2 and HCT-116 cells compared to either NO donor or MEK inhibitor alone. Cell invasion was determined using BioCoat Matrigel invasion chambers. MIAPaCa-2 cells (A and B), or HCT-116 cells (C and D) were placed in the upper chambers. Conditioned medium from NIH 3T3 cells was used as a chemoattractant. A and C show stained cancer cells, that migrated. Data shown are the results of triplicate experiments (B and D). Error bars indicate the standard errors of the means. †P<0.01, compared to GSNO alone; *P<0.01, compared to U0126 alone.

(Fig. 5D and E). The combination of NO donor (500 μM) and MEK inhibitor (10 μM) decreased the proliferation of HCT-116 cells compared to either NO donor or MEK inhibitor alone when the cells were incubated with EGF (Fig. 5F).

The combination of NO donor and MEK inhibitor decreases cancer cell invasion compared to either NO donor or MEK inhibitor alone. In the invasion assay, the addition of GSNO (200 μM) alone and U0126 (10 μM) alone reduced the invasion of MIAPaCa-2 and HCT-116 cells. The combination of GSNO (200 μM) and U0126 (10 μM) decreased the invasion of MIAPaCa-2 and HCT-116 compared to either GSNO (200 μM) or U0126 (10 μM) alone (Fig. 6A-D).

Discussion

In this study, we demonstrated that the combination of NO donor and MEK inhibitor inhibits both the PI3K/Akt and MEK/ERK pathways, and thus inhibits the proliferation and invasion of cancer cells. In contrast, GSNO alone upregulates MAPK pathway, although GSNO alone inhibits PI3K/Akt pathway. U0126 alone upregulates PI3K/Ak pathway, although U0126 inhibits MEK/ERK pathway. Fig. 7 illustrates our hypothesis on the molecular mechanism underlying the synergistic effect of the combination treatment with NO donor and MEK inhibitor in cancer cells.

IGF-I and EGF signaling play important roles in the proliferation and invasion of MIAPaCa-2 and HCT-116 cells, consistent with previous reports (1-3,24,25). IGF-IR and EGFR are expressed in various cancer cells, as we showed in this study. The MEK/ERK and PI3K/Akt pathways are two major pathways of IGF-I and EGF. Recent studies *in vitro* and *in vivo* suggest that antitumor therapy for K-Ras-mutant tumors requires dual inhibition of the MEK and PI3K pathways to achieve inhibition of tumor growth (26-28). The treatment that we propose is the dual inhibition of MAPK and PI3K pathways. NO inhibits IGF-IR and EGFR activity, as reported previously (29,30). Furthermore, NO induces the degradation of IRS-1 protein and the phosphorylation of IRS-1 (14,29,30). In addition, *Yasukawa et al* reported that NO directly modifies Akt protein and inhibits its activity (11). Recent studies have shown that NO inhibits cell proliferation and induces apoptosis in various cells including cancer cells, *in vitro* and *in vivo* (14-21).

Ras regulates multiple intracellular signaling pathways, of which the best understood is the Ras-RAF-MEK-ERK pathway. Substantial efforts made over the years to target the activated Ras protein have been unsuccessful and the downstream kinases in the Ras cascade remain attractive as therapeutic targets (31). Consequently, intensive preclinical and clinical research has led to the development of small molecule kinase inhibitors of its downstream effector MEK. In most pancreatic cancers, and in approximately 35 to 40% of colorectal cancer, K-Ras is activated due to mutations (32,33). K-Ras mutations in MIAPaCa-2 and HCT-116 cells, have been reported previously (34,35). Specific MEK1/2 inhibitors can inhibit the expression of phospho-ERK1/2 for various lengths of time *in vitro* (36-38). CI-1040, a MEK1/2 inhibitor, reduced tumor growth by 31.3% in mice inoculated with papillary thyroid carcinoma (PTC) cells carrying a BRAF mutation and by 47.5% in mice inoculated with PTC cells bearing a RET/

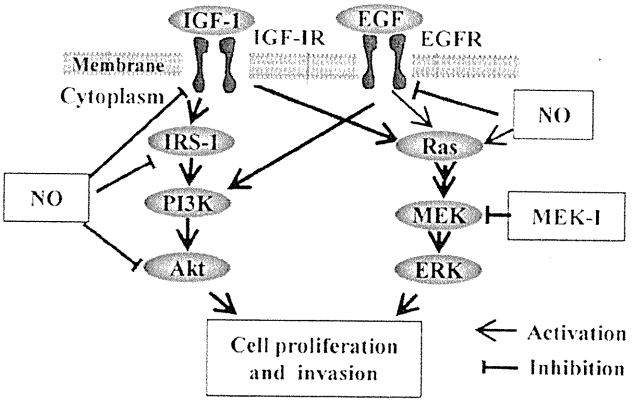

Figure 7. Schematic representation of our hypothesis on the molecular mechanism. The combination treatment of NO donor and MEK inhibitor downregulates PI3-K and MAPK pathways in cancer cells.

PTC1 rearrangement (39). Cl-1040 has been tested in other cancers, including colon cancer, breast cancer, non-small cell lung cancer (NSCLC), and melanoma, and was well tolerated by patients in phase I-II trials (40,41). NO donor upregulates phosphorylation of ERK1/2, although NO donor downregulates the PI3K/Akt pathway. In the present study, we showed that the phosphorylation of ERK1/2 is upregulated by NO donor without the stimulating of growth factors in MIAPaCa-2 and HCT-116 cells. These results are in accordance with previous studies reporting that NO directly modifies H-Ras and N-Ras through S-nitrosylation, resulting in the activation of their signaling (22,42). The present study showed that U0126 completely inhibits phosphorylation of ERK1/2, although U0126 upregulates IGF-I- and EGF-stimulated Akt phosphorylation (Figs. 1 and 2). These results are in accordance with previous reports (43,44). Furthermore, we showed that U0126 upregulates IGF-I- and EGF-stimulated phosphorylation of IGF-IR and EGFR. The U0126-induced upregulation of Akt phosphorylation may be explained by the upregulated phosphorylation of IGF-IR and EGFR. We surmise that a negative feedback mechanism from the inhibition of ERK activity may regulate this phenomenon. As described above, NO inhibits U0126-induced upregulated IGF-IR, EGFR, and Akt phosphorylation. These results suggest that the combination of NO donor and MEK inhibitor may be more effective in cancer therapy.

The usefulness of cancer therapy using NO, including inducible NO synthase gene therapy and administration of NO donor, was recently confirmed in animal models (45-47). Consequently, NO therapy has received considerable attention and is currently undergoing clinical evaluation for cancer prevention (48). On the other hand, MEK inhibitor is also feasible for cancer therapy (40,41). We believe that combined treatment of NO donor and MEK inhibitor may be an effective and promising strategy for cancer treatment.

Acknowledgements

This study was supported by Grant-in-Aid for Scientific Research (grant nos. 18591517 and 20591633) from the Japanese Society for the Promotion of Science.

References

1. Bergmann U, Funatomi H, Yokoyama M, Beger HG and Korc M: Insulin-like growth factor I overexpression in human pancreatic cancer: evidence for autocrine and paracrine roles. Cancer Res 55: 2007-2011, 1995.
2. Furukawa M, Raffeld M, Mateo C, *et al*: Increased expression of insulin-like growth factor I and/or its receptor in gastrinomas is associated with low curability, increased growth, and development of metastases. Clin Cancer Res 11: 3233-3242, 2005.
3. Kim HJ, Litzenburger BC, Cui X, *et al*: Constitutively active type I insulin-like growth factor receptor causes transformation and xenograft growth of immortalized mammary epithelial cells and is accompanied by an epithelial-to-mesenchymal transition mediated by NF-kappaB and snail. Mol Cell Biol 27: 3165-3175, 2007.
4. Salomon DS, Brandt R, Ciardiello F and Normanno N: Epidermal growth factor-related peptides and their receptors in human malignancies. Crit Rev Oncol Hematol 19: 183-232, 1995.
5. Normanno N, Bianco C, De Luca A, Maiello MR and Salomon DS: Target-based agents against ErbB receptors and their ligands: a novel approach to cancer treatment. Endocr Relat Cancer 10: 1-21, 2003.
6. Ito T, Sasaki Y and Wands JR: Overexpression of human insulin receptor substrate 1 induces cellular transformation with activation of mitogen-activated protein kinases. Mol Cell Biol 16: 943-951, 1996.
7. Tanaka S and Wands JR: A carboxy-terminal truncated insulin receptor substrate-1 dominant negative protein reverses the human hepatocellular carcinoma malignant phenotype. J Clin Invest 98: 2100-2108, 1996.
8. Park HS, Huh SH, Kim MS, Lee SH and Choi EJ: Nitric oxide negatively regulates c-Jun N-terminal kinase/stress-activated protein kinase by means of S-nitrosylation. Proc Natl Acad Sci USA 97: 14382-14387, 2000.
9. Reynaert NL, Ckless K, Korn SH, *et al*: Nitric oxide represses inhibitory kappaB kinase through S-nitrosylation. Proc Natl Acad Sci USA 101: 8945-8950, 2004.
10. Mannick JB, Hausladen A, Liu L, *et al*: Fas-induced caspase denitrosylation. Science 284: 651-654, 1999.
11. Yasukawa T, Tokunaga E, Ota H, Sugita H, Martyn JA and Kaneki M: S-nitrosylation-dependent inactivation of Akt/protein kinase B in insulin resistance. J Biol Chem 280: 7511-7518, 2005.
12. Ambs S, Merriam WG, Ogunfusika MO, *et al*: p53 and vascular endothelial growth factor regulate tumor growth of NOS2-expressing human carcinoma cells. Nat Med 4: 1371-1376, 1998.
13. Camp ER, Yang A, Liu W, *et al*: Roles of nitric oxide synthase inhibition and vascular endothelial growth factor receptor-2 inhibition on vascular morphology and function in an in vivo model of pancreatic cancer. Clin Cancer Res 12: 2628-2633, 2006.
14. Sugita H, Kaneki M, Furuhashi S, Hirota M, Takamori H and Baba H: Nitric oxide inhibits the proliferation and invasion of pancreatic cancer cells through degradation of insulin receptor substrate-1 protein. Mol Cancer Res 8: 1152-1163, 2010.
15. Kalivendi SV, Kotamraju S, Zhao H, Joseph J and Kalyanaraman B: Doxorubicin-induced apoptosis is associated with increased transcription of endothelial nitric-oxide synthase. Effect of antiapoptotic antioxidants and calcium. J Biol Chem 276: 47266-47276, 2001.
16. Wang B, Wei D, Crum VE, *et al*: A novel model system for studying the double-edged roles of nitric oxide production in pancreatic cancer growth and metastasis. Oncogene 22: 1771-1782, 2003.
17. Peshes-Yaloz N, Rosen D, Sondel PM, Krammer PH and Berke G: Up-regulation of Fas (CD95) expression in tumour cells in vivo. Immunology 120: 502-511, 2007.
18. Kotamraju S, Williams CL and Kalyanaraman B: Statin-induced breast cancer cell death: role of inducible nitric oxide and arginase-dependent pathways. Cancer Res 67: 7386-7394, 2007.
19. Notas G, Nifli AP, Kampa M, Vercauteren J, Kouroumalis E and Castanas E: Resveratrol exerts its antiproliferative effect on HepG2 hepatocellular carcinoma cells, by inducing cell cycle arrest, and NOS activation. Biochim Biophys Acta 1760: 1657-1666, 2006.
20. Jarry A, Charrier L, Bou-Hanna C, *et al*: Position in cell cycle controls the sensitivity of colon cancer cells to nitric oxide-dependent programmed cell death. Cancer Res 64: 4227-4234, 2004.
21. Chawla-Sarkar M, Bauer JA, Lupica JA, *et al*: Suppression of NF-kappa B survival signaling by nitrosylcobalamin sensitizes neoplasms to the anti-tumor effects of Apo2L/TRAIL. J Biol Chem 278: 39461-39469, 2003.
22. Lim KH, Ancrile BB, Kashatus DF and Counter CM: Tumour maintenance is mediated by eNOS. Nature 452: 646-649, 2008.
23. Shields JM, Pruitt K, McFall A, Shaub A and Der CJ: Understanding Ras: 'it ain't over 'til it's over'. Trends Cell Biol 10: 147-154, 2000.
24. Van der Heyden MA, van Bergen en Henegouwen PM, De Ruiter N, *et al*: The actin binding domain of the epidermal growth factor receptor is required for EGF-stimulated tissue invasion. Exp Cell Res 234: 521-526, 1997.
25. Baselga J and Arteaga CL: Critical update and emerging trends in epidermal growth factor receptor targeting in cancer. J Clin Oncol 23: 2445-2459, 2005.
26. Engelman JA, Chen L, Tan X, *et al*: Effective use of PI3K and MEK inhibitors to treat mutant Kras G12D and PIK3CA H1047R murine lung cancers. Nat Med 14: 1351-1356, 2008.
27. Wee S, Jagani Z, Xiang KX, *et al*: PI3K pathway activation mediates resistance to MEK inhibitors in KRAS mutant cancers. Cancer Res 69: 4286-4293, 2009.
28. Yu K, Toral-Barza L, Shi C, Zhang WG and Zask A: Response and determinants of cancer cell susceptibility to PI3K inhibitors: combined targeting of PI3K and Mek1 as an effective anticancer strategy. Cancer Biol Ther 7: 307-315, 2008.
29. Murillo-Carretero M, Torroglosa A, Castro C, Villalobo A and Estrada C: S-Nitrosylation of the epidermal growth factor receptor: a regulatory mechanism of receptor tyrosine kinase activity. Free Radic Biol Med 46: 471-479, 2009.
30. Studer RK: Nitric oxide decreases IGF-1 receptor function in vitro; glutathione depletion enhances this effect in vivo. Osteoarthritis Cartilage 12: 863-869, 2004.
31. Sebolt-Leopold JS: Advances in the development of cancer therapeutics directed against the RAS-mitogen-activated protein kinase pathway. Clin Cancer Res 14: 3651-3656, 2008.
32. Almoguera C, Shibata D, Forrester K, Martin J, Arnheim N and Perucho M: Most human carcinomas of the exocrine pancreas contain mutant c-K-ras genes. Cell 53: 549-554, 1988.
33. Bos JL, Fearon ER, Hamilton SR, *et al*: Prevalence of ras gene mutations in human colorectal cancers. Nature 327: 293-297, 1987.
34. Bocci G, Fioravanti A, Orlandi P, *et al*: Fluvastatin synergistically enhances the antiproliferative effect of gemcitabine in human pancreatic cancer MIAPaCa-2 cells. Br J Cancer 93: 319-330, 2005.
35. Allgayer H, Wang H, Shirasawa S, Sasazuki T and Boyd D: Targeted disruption of the K-ras oncogene in an invasive colon cancer cell line down-regulates urokinase receptor expression and plasminogen-dependent proteolysis. Br J Cancer 80: 1884-1891, 1999.
36. Favata MF, Horiuchi KY, Manos EJ, *et al*: Identification of a novel inhibitor of mitogen-activated protein kinase kinase. J Biol Chem 273: 18623-18632, 1998.
37. Liu D, Liu Z, Jiang D, Dackiw AP and Xing M: Inhibitory effects of the mitogen-activated protein kinase kinase inhibitor CI-1040 on the proliferation and tumor growth of thyroid cancer cells with BRAF or RAS mutations. J Clin Endocrinol Metab 92: 4686-4695, 2007.
38. Henderson YC, Fredrick MJ and Clayman GL: Differential responses of human papillary thyroid cancer cell lines carrying the RET/PTC1 rearrangement or a BRAF mutation to MEK1/2 inhibitors. Arch Otolaryngol Head Neck Surg 133: 810-815, 2007.
39. Henderson YC, Ahn SH and Clayman GL: Inhibition of the growth of papillary thyroid carcinoma cells by CI-1040. Arch Otolaryngol Head Neck Surg 135: 347-354, 2009.
40. Haura EB, Ricart AD, Larson TG, *et al*: A phase II study of PD-0325901, an oral MEK inhibitor, in previously treated patients with advanced non-small cell lung cancer. Clin Cancer Res 16: 2450-2457, 2010.
41. LoRusso PM, Krishnamurthi SS, Rinehart JJ, *et al*: Phase I pharmacokinetic and pharmacodynamic study of the oral MAPK/ERK kinase inhibitor PD-0325901 in patients with advanced cancers. Clin Cancer Res 16: 1924-1937, 2010.
42. Ibiza S, Perez-Rodriguez A, Ortega A, *et al*: Endothelial nitric oxide synthase regulates N-Ras activation on the Golgi complex of antigen-stimulated T cells. Proc Natl Acad Sci USA 105: 10507-10512, 2008.

43. Yu CF, Liu ZX and Cantley LG: ERK negatively regulates the epidermal growth factor-mediated interaction of Gab1 and the phosphatidylinositol 3-kinase. J Biol Chem 277: 19382-19388, 2002.
44. Yoon YK, Kim HP, Han SW, *et al*: Combination of EGFR and MEK1/2 inhibitor shows synergistic effects by suppressing EGFR/HER3-dependent AKT activation in human gastric cancer cells. Mol Cancer Ther 8: 2526-2536, 2009.
45. Adams C, McCarthy HO, Coulter JA, *et al*: Nitric oxide synthase gene therapy enhances the toxicity of cisplatin in cancer cells. J Gene Med 11: 160-168, 2009.
46. Kiziltepe T, Hideshima T, Ishitsuka K, *et al*: JS-K, a GST-activated nitric oxide generator, induces DNA double-strand breaks, activates DNA damage response pathways, and induces apoptosis in vitro and in vivo in human multiple myeloma cells. Blood 110: 709-718, 2007.
47. Wang Z, Cook T, Alber S, *et al*: Adenoviral gene transfer of the human inducible nitric oxide synthase gene enhances the radiation response of human colorectal cancer associated with alterations in tumor vascularity. Cancer Res 64: 1386-1395, 2004.
48. Ma Q, Wang Y, Gao X, Ma Z and Song Z: L-arginine reduces cell proliferation and ornithine decarboxylase activity in patients with colorectal adenoma and adenocarcinoma. Clin Cancer Res 13: 7407-7412, 2007.

Ann Surg Oncol
DOI 10.1245/s10434-011-2176-3

Annals of
SURGICAL ONCOLOGY
OFFICIAL JOURNAL OF THE SOCIETY OF SURGICAL ONCOLOGY

ORIGINAL ARTICLE – TRANSLATIONAL RESEARCH AND BIOMARKERS

Pyrosequencing Assay to Measure LINE-1 Methylation Level in Esophageal Squamous Cell Carcinoma

Shiro Iwagami, MD, Yoshifumi Baba, MD, PhD, Masayuki Watanabe, MD, PhD, Hironobu Shigaki, MD, Keisuke Miyake, MSc, Satoshi Ida, MD, PhD, Yohei Nagai, MD, Takatsugu Ishimoto, MD, PhD, Masaaki Iwatsuki, MD, PhD, Yasuo Sakamoto, MD, PhD, Yuji Miyamoto, MD, PhD, and Hideo Baba, MD, PhD

Department of Gastroenterological Surgery, Graduate School of Medical Science, Kumamoto University, Kumamoto, Japan

ABSTRACT

Background. Genome-wide DNA hypomethylation plays a role in genomic instability and carcinogenesis. DNA methylation in the long interspersed nucleotide element 1 L1 (LINE-1) repetitive element is a good indicator of global DNA methylation level. LINE-1 methylation is a useful marker for predicting cancer prognosis and monitoring efficacy of adjuvant therapy. Nonetheless, no study has examined LINE-1 methylation in esophageal squamous cell carcinoma (ESCC). The aim of this study is to assess the precision of sodium bisulfite conversion and polymerase chain reaction (PCR) pyrosequencing assay for evaluating LINE-1 methylation in ESCC.

Methods. To measure assay precision, we performed bisulfite conversion on 5 different DNA specimen aliquots (bisulfite-to-bisulfite) and repeated PCR pyrosequencing five times (run to run). Second, to assess heterogeneity of LINE-1 methylation levels within tumor, we made 5 different tissue sections from one tumor and examined LINE-1 methylation level of each section (section to section). Third, to evaluate LINE-1 methylation status in ESCC, we applied this assay to 30 ESCCs and 30 matched normal esophageal mucosa.

Results. Bisulfite-to-bisulfite standard deviation (SD) ranged from 1.44 to 2.90 (median 2.32) in ESCCs; and 0.57 to 4.02 (median 1.23) in normal esophagus. Run-to-run SD ranged from 0.63 to 3.25 (median 1.54) in ESCCs. Section-to-section SD ranged from 1.37 to 3.31 (median 1.94). ESCC tissues showed significantly lower levels of LINE-1 methylation than matched normal mucosa ($P < .0001$; $n = 30$). There was no significant relationship between LINE-1 methylation level and tumor stage ($P = 0.14$).

Conclusions. Bisulfite conversion and PCR pyrosequencing assay can measure LINE-1 methylation in ESCC, and may be useful in clinical and research settings.

Esophageal squamous cell carcinoma (ESCC), the major histologic type of esophageal cancer in East Asia, is one of the most aggressive malignant tumors.[1] Despite the development of multimodality therapies including surgery, chemotherapy, radiotherapy, and chemoradiotherapy, prognosis even of patients who underwent complete resection of their carcinomas remains poor.[2–4] Limited improvement in treatment outcomes by conventional therapies urges us to seek innovative strategies for treating ESCC, especially those that are molecular targeted. Importantly, epigenetic changes, including DNA methylation alterations, are reversible and can thus be targets for therapy or chemoprevention.[5,6]

DNA methylation is a major epigenetic mechanism in X chromosome inactivation, imprinting and repression of transposable elements and endogenous retroviral sequences.[5–7] Global DNA hypomethylation appears to play an important role in genomic instability, leading to cancer development.[8–10] Because long interspersed nucleotide element 1 L1 (LINE-1) retrotransposon constitutes a substantial portion (approximately 17%) of the human genome, the methylation status of LINE-1 reflects the global DNA methylation level.[11] In some types of human neoplasms, LINE-1 methylation has been shown to be highly variable, and LINE-1 hypomethylation is strongly associated with poor prognosis.[12–15] There is a significant correlation of LINE-1 methylation levels within synchronous colorectal

First Received: 27 July 2011

H. Baba, MD, PhD
e-mail: hdobaba@kumamoto-u.ac.jp

Published online: 21 December 2011

cancer pairs (i.e., 2 or more primary tumors in one patient), suggesting the presence of genetic and/or environmental factors influencing LINE-1 methylation levels that are unlikely the result of a purely stochastic phenomenon.[16] Thus, LINE-1 methylation status in human cancer tissues is increasingly important for better understanding of epigenetic alterations during the carcinogenic process. Although there is interesting evidence to suggest that promoter hypermethylation, particularly of tumor suppressor genes (e.g., *CDKN2A*, *FHIT*, *MGMT*), is a critical early step in esophageal tumorigenesis, to our knowledge, no study has examined global DNA hypomethylation (i.e., LINE-1 methylation level) in ESCC.[17–19]

In this study, we assessed the precision of sodium bisulfite conversion and polymerase chain reaction (PCR) pyrosequencing assay for evaluating LINE-1 methylation level in ESCC. Second, we evaluated LINE-1 methylation level in 30 paraffin-embedded ESCC specimens and 30 matched normal esophageal specimens. We have shown that LINE-1 methylation level in ESCC is highly variable and LINE-1 methylation level in cancer specimens is significantly lower than that in normal specimens.

MATERIALS AND METHODS

Study Group

The present study involved formalin-fixed, paraffin-embedded ESCC specimens of 30 cases [tumor, node, metastasis system classification stage I (IA and IB): 10 cases, stage II (IIA and IIB): 10 cases, stage III (IIIA, IIIB and IIIC): 10 cases] and 30 matched paraffin-embedded normal esophageal specimens. Tumor staging was done according to the American Joint Committee on Cancer Staging Manual (7th edition).[20] These specimens were obtained by surgical resection at Kumamoto University Hospital. None of these patients underwent preoperative chemotherapy, preoperative radiotherapy, or preoperative chemoradiotherapy. For the precision of sodium bisulfite conversion and PCR pyrosequencing assay, 4 cases were randomly extracted from these 30 cases. Informed consent for the research was obtained from each patient. The study design was approved by the ethics review board of our university.

Hematoxylin and Eosin Staining, DNA Extraction, and Sodium Bisulfite Treatment

Hematoxylin and eosin (H&E) staining protocol is as follows: (1) Bake slide for 2 h at 58°C. (2) Deparaffinize sections in 3 changes of xylene, 2 min each. (3) Rehydrate in 3 changes of absolute alcohol, 2 min each, and in 95% alcohol for 1 min. (4) Wash briefly in distilled water. (5) Stain in Harris hematoxylin solution for 3 min. (6) Wash in running tap water for 3 min. (7) Blue in 0.2% ammonia water for 30 s. (8) Wash in running tap water for 5 min. (9) Rinse in 80% alcohol for 15 s, in 95% alcohol for 15 s, and in 10% alcohol for 15 s. (10) Counterstain in eosin–phloxine B solution for 15 s. (11) Dehydrate in 100% alcohol for 5 min. (12) Clear in 2 changes of xylene, 2 min each.

H&E-stained slides of the tumors were reviewed by one pathologist, and areas of tumor and normal mucosa were marked. H&E-stained tissue sections (depending on tissue and tumor size, in average, large tumor tissue 10 μm × 1 section) from each case were scraped off slides for DNA extraction. Genomic DNA extraction from tumor and normal mucosa and sodium bisulfite treatment on genomic DNA were performed as previously described by Ogino et al..[21,22]

Pyrosequencing to Measure LINE-1 Methylation

LINE-1 methylation level measured by Pyrosequencing is a good indicator of cellular 5-methylcytosine level (i.e., global DNA methylation level).[23,24] PCR and subsequent pyrosequencing for LINE-1 were performed as previously described by Ogino et al. with the PyroMark kit (Qiagen).[12,25–27] This assay amplifies a region of LINE-1 element (position 305 to 331 in accession no. X58075), which includes 4 CpG cites. The PCR condition was 45 cycles of 95°C for 20 s, 50°C for 20 s, and 72°C for 20 s, followed by 72°C for 5 min. The biotinylated PCR product was purified and made single-stranded to act as a template in a pyrosequencing reaction with the Pyrosequencing Vacuum Prep Tool (Qiagen). Pyrosequencing reactions were performed in the PyroMark Q24 System (Qiagen). The nucleotide dispensation order was: ACT CAG TGT GTC AGT CAG TTA GTC TG. The non-CpG cytosine in LINE-1 repetitive sequences has been documented to be rarely methylated. Thus, complete conversion of cytosine at a non-CpG site ensured successful bisulfite conversion. The amount of C relative to the sum of the amounts of C and T at each CpG site was calculated as percentage (i.e., 0 to 100). The average of the relative amounts of C in the 4 CpG sites was used as overall LINE-1 methylation level in a given tumor (Fig. 1).

Statistical Analysis

We used the JMP program, version 9 (SAS Institute, Cary, NC), for all statistical analyses. All *P* values were 2-sided. To compare mean LINE-1 methylation levels, we performed the paired *t*-test for variables with 2 categories

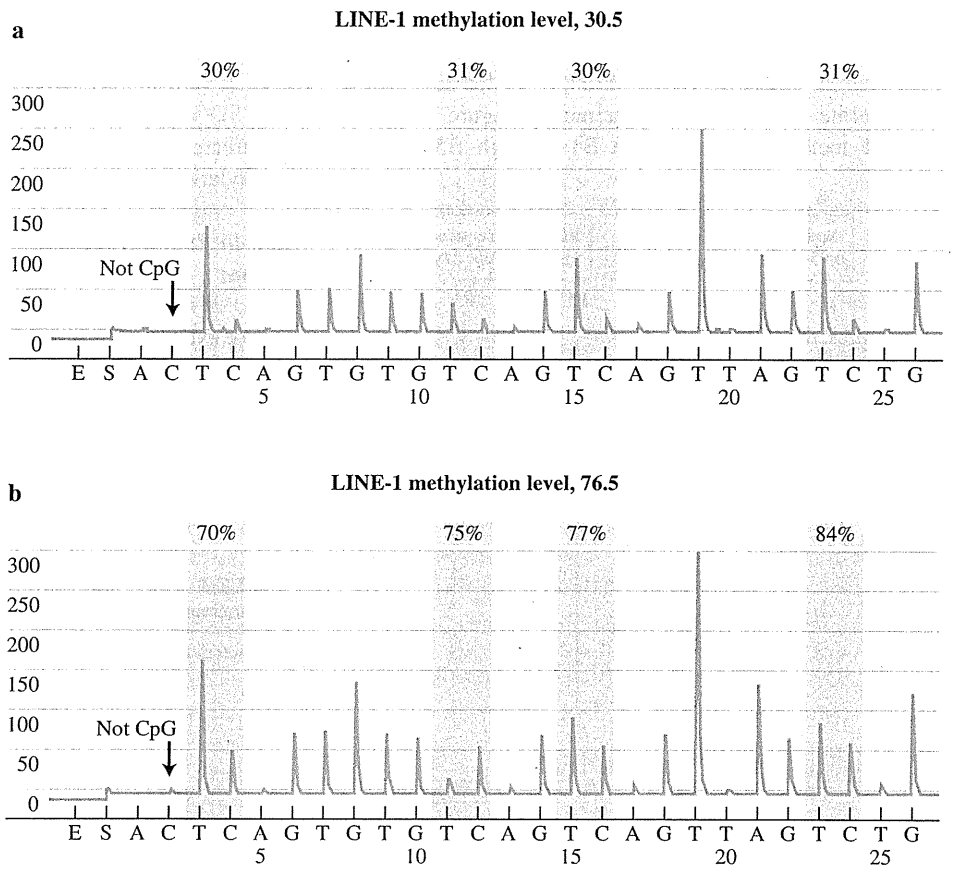

FIG. 1 Pyrosequencing to measure LINE-1 methylation. **a** LINE-1 hypomethylated tumor (methylation level, 30.5). **b** LINE-1 hypermethylated tumor (methylation level, 76.5). The percentages (*blue*) are the proportion of C at each CpG site after bisulfite conversion, and the methylation level of each CpG site is estimated by the proportion of C (%). An overall LINE-1 methylation level is calculated as the average of the proportions of C (%) at the 4 CpG sites. The first, third, and fourth CpG sites follow mononucleotide T repeats, resulting in higher T peaks than the second CpG site, and the proportion of C (%) has been adjusted accordingly. The *arrows* indicate no residual C at the non-CpG site, ensuring complete bisulfite conversion

or the ANOVA test for variables with more than 2 categories.

RESULTS

Strategy to Assess Precision of Bisulfite Conversion and PCR Pyrosequencing

To assess precision of bisulfite-PCR pyrosequencing for LINE-1 methylation, we used 4 paraffin-embedded ESCC specimens and 4 matched paraffin-embedded normal esophageal specimens. Figure 2a illustrates our overall strategy to measure the precision of bisulfite DNA conversion and PCR pyrosequencing on each specimen. We performed bisulfite conversion on 5 different aliquots from each specimen on 5 different days. Thus, from each specimen, we have 5 different bisulfite-converted DNA specimens (designated as B1 through B5), which ideally should show at least similar levels of LINE-1 methylation. By means of PCR pyrosequencing assay, we measured LINE-1 methylation level in each of the 5 separate bisulfite-converted DNA specimens. For each case, we measured the standard deviation (SD) of these 5 LINE-1 methylation levels on B1 through B5, which would depend on variations in bisulfite conversion and PCR pyrosequencing. Furthermore, we repeated PCR pyrosequencing assays five times (designated as P1 through P5) on 2 (B1 and B2) of the 5 bisulfite-converted DNA specimens, on 5 different days. We calculated the SD of the 5 LINE-1 methylation levels (P1 through P5) on one bisulfite-converted DNA specimen. This SD would primarily depend on run-to-run (between-run) variation of PCR pyrosequencing assay, but not on bisulfite conversion.

Table 1 shows an example of patient 1 in the assessment of precision of LINE-1 methylation measurement. Each of B1 though B5 represents each bisulfite-converted DNA specimen from this case. We obtained mean LINE-1 methylation value (61.4) across B1 through B5 in a single PCR pyrosequencing run, and calculated bisulfite-to-bisulfite SD (1.44). P1 though P5 represent results of PCR pyrosequencing assay by 5 repeats on 5 different days. Mean LINE-1 methylation value was 61.9 with SD of 0.67 for B1 specimen in this case.

Bisulfite-to-Bisulfite SD of LINE-1 Methylation Values

Each of the 4 esophageal cancers and 4 normal esophageal epitheliums was treated by sodium bisulfite on 5

different days, and aliquoted into 5 different tubes (B1 through B5) (Fig. 2a). We assessed variation of LINE-1 methylation values across B1 through B5 for each source of bisulfite-treated DNA specimens. Figure 3a shows LINE-1 methylation values on B1 through B5 for each specimen source. The SD of normal tissue and tumor tissue was as follows: 0.57 and 1.44 in case 1; 0.65 and 2.44 in case 2; 1.80 and 2.19 in case 3; and 4.02 and 2.89 in case 4. The SD was generally small, implying that a single bisulfite-treated DNA aliquot could provide precise LINE-1 methylation measurement.

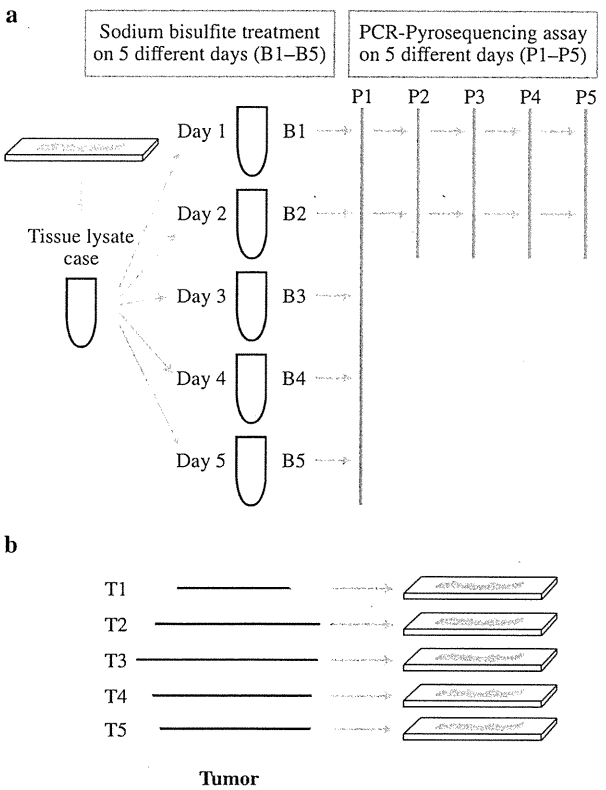

FIG. 2 **a** Example (in patient 1) of a strategy to assess precision of bisulfite conversion and PCR pyrosequencing on each specimen. Bisulfite conversion was performed on 5 different aliquots (B1–B5) from each specimen. PCR pyrosequencing was performed on the 5 bisulfite-treated specimens (B1–B5) and was repeated five times on 2 specimens (B1 and B2) on 5 different days (P1–P5). **b** Strategy to assess location-specific LINE-1 methylation levels and/or heterogeneity of LINE-1 methylation levels within tumor. Five different tissue sections (T1–T5) were made from 1 tumor, and PCR pyrosequencing was performed on these 5 different tissue sections (T1–T5)

Run-to-Run (Between-Run) SD of LINE-1 Methylation Values

We examined run-to-run (between-run) variation of PCR pyrosequencing assay by repeating five times by using 2 of the 5 bisulfite-treated DNA specimens from esophageal cancers (Fig. 2a). Figure 3b shows LINE-1 methylation value of 5 different PCR pyrosequencing runs on various specimens. The SD was as follows: 0.67 for B1 of patient 1's

TABLE 1 Assessment of precision of LINE-1 methylation measurement

Characteristic	Different PCR pyrosequencing runs (on 5 different days)						
	P1	P2	P3	P4	P5	Mean of LINE-1 methylation values	Run-to-run SD
Different bisulfite-treated DNA specimens							
B1	61.0	62.5	61.4	62.5	62.3	61.9	0.67
B2	60.3	62.8	61.8	64.4	63.8	62.6	1.65
B3	62.5						
B4	60.0						
B5	63.3						
Mean of LINE-1 methylation values	61.4						
Bisulfite-to-bisulfite SD	1.44						

Example from tumor from patient 1

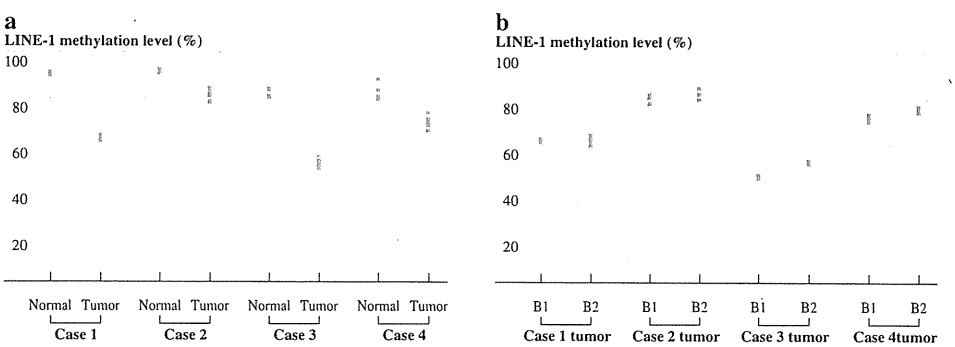

FIG. 3 Results on repeated measurements of LINE-1 methylation levels. **a** Bisulfite-to-bisulfite variation of LINE-1 methylation values. **b** Run-to-run variation of LINE-1 methylation values

TABLE 2 Assessment of location-specific LINE-1 methylation levels and/or heterogeneity of LINE-1 methylation levels within tumor

Patient no.	Different tissue sections from one tumor						
	T1	T2	T3	T4	T5	Mean of LINE-1 methylation values	Section-to-section SD
1	64.2	62.7	60.0	61.4	61.0	61.9	1.63
2	78.9	75.3	78.5	71.9	72.3	75.4	3.31
3	52.7	52.5	53.1	55.4	51.8	53.1	1.37
4	73.6	68.2	69.5	72.8	70.9	71.0	2.24

tumor: 1.65 for B2 of patient 1's tumor: 1.42 for B1 of patient 2's tumor: 2.62 for B2 of patient 2's tumor: 0.63 for B1 of patient 3's tumor: 3.25 for B2 of patient 3's tumor: 1.27 for B1 of patient 4's tumor: and 2.91 for B2 of patient 4's tumor.

Section-to-Section SD of LINE-1 Methylation Values

To assess location-specific LINE-1 methylation levels and/or heterogeneity of LINE-1 methylation levels within tumor, we examined section-to-section variation of PCR pyrosequencing assay by making 5 different tissue sections from one tumor (patients 1, 2, 3, or 4) (Fig. 2b). The section-to-section SD was relatively small (patient 1, 1.63; patient 2, 3.31; patient 3, 1.37; patient 4, 2.24) (Table 2). The median value of section-to-section SD was 1.94.

LINE-1 Methylation Level in Esophageal Cancers

We examined LINE-1 methylation levels in 30 esophageal cancer tissues and matched normal esophageal mucosa. Cancer tissues showed significantly lower levels of LINE-1 methylation (median 71.5; mean 69.6; SD 14.5; range 30.5–92.4, all in 0–100 scale) than matched normal mucosa (median 89.9; mean 88.6; SD 3.4; range 80.8–93.5) ($P < 0.0001$) (Fig. 4a).

LINE-1 Methylation Level According to Tumor Stage

There was no significant relationship between LINE-1 methylation level and tumor stage (stage I: median 74.6; mean 74.0; SD 11.7, stage II: median 61.6; mean 62.8; SD 17.3, stage III: median 71.3; mean 73.2; SD 11.4) ($P = 0.14$) (Fig. 4b).

DISCUSSION

DNA methylation in the LINE-1 repetitive element is a good indicator of global DNA methylation level.[11] Given that LINE-1 methylation is likely a useful marker for predicting cancer prognosis and monitoring efficacy of adjuvant cancer therapy, a better understanding of LINE-1 methylation status in cancer tissues is of particular important.[12–14,28,29] To our knowledge, this is the first study evaluating LINE-1 methylation level in ESCC utilizing PCR pyrosequencing assay. Sodium bisulfite conversion and PCR pyrosequencing assay of LINE-1 methylation level had good precision for paraffin-embedded ESCC specimens. Second, different tissue sections from one tumor had similar LINE-1 methylation level, implying that LINE-1 methylation level of the representative tissue section likely represents that of the whole tumor. Third, ESCC tumors showed far lower levels of LINE-1 methylation than matched normal mucosa. Our findings indicate that LINE-1 methylation level in ESCC can be measured by bisulfite pyrosequencing assay for the future clinical or research use.

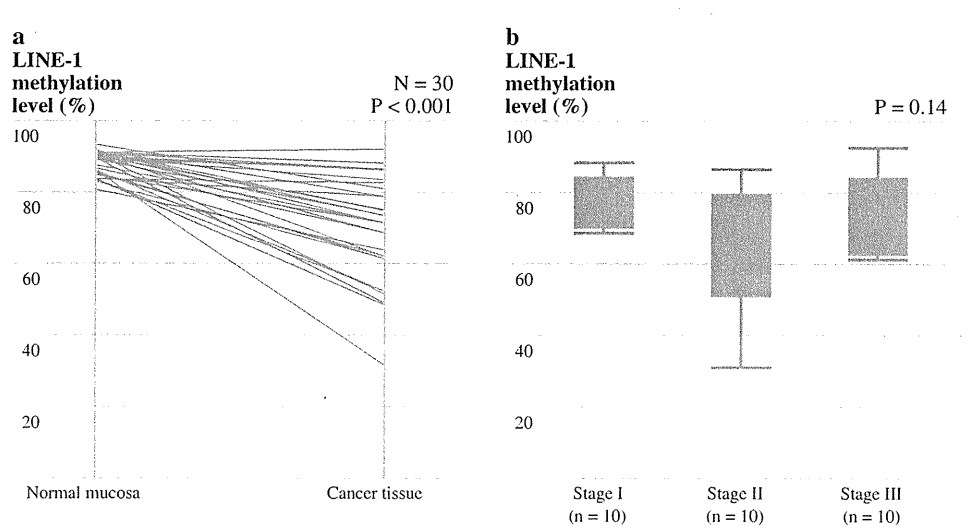

FIG. 4 **a** LINE-1 methylation levels in 30 colorectal cancers and matched normal mucosa. Cancer tissues showed a significantly lower level of methylation (mean 69.6; median 71.5) than matched normal mucosa (mean 88.6; median 89.9) ($P < 0.0001$). **b** LINE-1 methylation level according to tumor stage. There was no significant relationship between LINE-1 methylation level and tumor stage ($P = 0.14$)

Pyrosequencing is a nonelectrophoretic nucleotide extension sequencing technology for various applications including single nucleotide polymorphism genotyping, bacterial strain typing, mutation detection in tumors, and quantitative CpG island methylation analyses.[30,31] Pyrosequencing is a useful methodology in molecular diagnostics and large-scale epidemiologic studies.[32,33] Pyrosequencing has previously been shown to be more precise than combined bisulfite and restriction analysis and MethyLight for LINE-1 methylation measurements of plasma DNA.[34] Precision of pyrosequencing assay to measure LINE-1 methylation in colon cancer and normal colonic mucosa has been also reported.[26] Nonetheless, no study has evaluated its performance on ESCC tissues. First, to measure the precision of bisulfite conversion, we performed bisulfite treatment on 5 different aliquots of DNA from ESCCs and matched normal esophagus. Our results indicate that variation of LINE-1 methylation values between different bisulfite treatments is not substantial, and that one bisulfite-treated DNA specimen can provide precise measurement of LINE-1 methylation value. Second, to measure the precision of the PCR pyrosequencing assay, we also repeated PCR pyrosequencing five times. Our results indicate that run-to-run (between-run) variation of LINE-1 methylation values is not large, and a single run of PCR pyrosequencing can provide reasonably precise measurement of LINE-1 methylation in a given specimen. Third, to evaluate location-specific LINE-1 methylation levels and/or heterogeneity of LINE-1 methylation levels within tumor, we made 5 different tissue sections from one ESCC tumor and examined LINE-1 methylation of each section. Variation of LINE-1 methylation values between different tissue sections is relatively small, implying that LINE-1 methylation level of the representative tissue section likely represents that of the whole tumor. These findings collectively support the reliability of bisulfite pyrosequencing assay for assessing LINE-1 methylation level in ESCC.

In addition to the role as a surrogate marker for global DNA methylation, LINE-1 methylation status by itself likely has biological effects because retrotransposons such as LINE-1 elements can provide alternative promoters, and contribute to noncoding RNA expression that regulates functions of a number of genes.[35–37] Moreover, retrotransposons activated by DNA hypomethylation may transpose themselves throughout the genome, leading to gene disruptions and chromosomal instability.[38–40] Previous studies have reported that most carcinomas of colon, stomach, breast, lung, prostate, and liver show hypomethylation of LINE-1 compared with matched normal tissues.[41] In this study, we have demonstrated that ESCC tissues show far lower LINE-1 methylation levels than matched normal mucosa, which is in agreement with previous findings on other type of cancers. Interestingly, there was no significant relation between tumor stage and LINE-1 methylation level in ESCC. This finding may suggest that LINE-1 hypomethylation is an early event of esophageal squamous cell carcinogenesis. As this study is limited by small sample size ($n = 30$), further studies with large sample sizes are necessary to elucidate the exact relationship of LINE-1 hypomethylation (i.e., genome-wide DNA hypomethylation) with tumor development, progression, and growth in ESCC.

In summary, our study has shown that sodium bisulfite conversion is reproducible and that subsequent PCR pyrosequencing assay can assess LINE-1 methylation in ESCC. We currently plan further study focusing on the relationship between LINE-1 methylation, environmental risk factors (e.g., smoking, alcohol) and patient survival in ESCC.

ACKNOWLEDGMENT Supported in part by the Japan Society for the Promotion of Science (JSPS) Grant-in-Aid for Scientific Research (grant 23689061) and the Kobayashi Foundation for Cancer Research.

REFERENCES

1. Enzinger PC, Mayer RJ. Esophageal cancer. *N Engl J Med.* 2003;349:2241–52.
2. Kleinberg L, Forastiere AA. Chemoradiation in the management of esophageal cancer. *J Clin Oncol.* 2007;25:4110–7.
3. Wouters MW, Karim-Kos HE, le Cessie S, et al. Centralization of esophageal cancer surgery: does it improve clinical outcome? *Ann Surg Oncol.* 2009;16:1789–98.
4. Brucher BL, Swisher SG, Konigsrainer A, et al. Response to preoperative therapy in upper gastrointestinal cancers. *Ann Surg Oncol.* 2009;16:878–86.
5. Rodriguez-Paredes M, Esteller M. Cancer epigenetics reaches mainstream oncology. *Nat Med.* 2011;17:330–9.
6. Taby R, Issa JP. Cancer epigenetics. *CA Cancer J Clin.* 2011;60:376–92.
7. Jones PA, Baylin SB. The epigenomics of cancer. *Cell.* 2007;128:683–92.
8. Gaudet F, Hodgson JG, Eden A, et al. Induction of tumors in mice by genomic hypomethylation. *Science.* 2003;300:489–92.
9. Holm TM, Jackson-Grusby L, Brambrink T, Yamada Y, Rideout WM 3rd, Jaenisch R. Global loss of imprinting leads to widespread tumorigenesis in adult mice. *Cancer Cell.* 2005;8:275–85.
10. Suzuki K, Suzuki I, Leodolter A, et al. Global DNA demethylation in gastrointestinal cancer is age dependent and precedes genomic damage. *Cancer Cell.* 2006;9:199–207.
11. Cordaux R, Batzer MA. The impact of retrotransposons on human genome evolution. *Nat Rev Genet.* 2009;10:691–703.
12. Ogino S, Nosho K, Kirkner GJ, et al. A cohort study of tumoral LINE-1 hypomethylation and prognosis in colon cancer. *J Natl Cancer Inst.* 2008;100:1734–8.
13. Saito K, Kawakami K, Matsumoto I, Oda M, Watanabe G, Minamoto T. Long interspersed nuclear element 1 hypomethylation is a marker of poor prognosis in stage IA non–small cell lung cancer. *Clin Cancer Res.* 2010;16:2418–26.
14. Sigalotti L, Fratta E, Bidoli E, et al. Methylation levels of the "long interspersed nucleotide element-1" repetitive sequences predict survival of melanoma patients. *J Transl Med.* 2011;9:78.

15. Zhang C, Xu Y, Zhao J, et al. Elevated expression of the stem cell marker CD133 associated with line-1 demethylation in hepatocellular carcinoma. *Ann Surg Oncol.* 2011;18:2373–80.
16. Nosho K, Kure S, Irahara N, et al. A prospective cohort study shows unique epigenetic, genetic, and prognostic features of synchronous colorectal cancers. *Gastroenterology.* 2009;137: 1609–20.
17. Maesawa C, Tamura G, Nishizuka S, et al. Inactivation of the *CDKN2* gene by homozygous deletion and de novo methylation is associated with advanced stage esophageal squamous cell carcinoma. *Cancer Res.* 1996;56:3875–8.
18. Kuroki T, Trapasso F, Yendamuri S, et al. Allele loss and promoter hypermethylation of VHL, RAR-beta, RASSF1A, and FHIT tumor suppressor genes on chromosome 3p in esophageal squamous cell carcinoma. *Cancer Res.* 2003;63:3724–8.
19. Wang J, Sasco AJ, Fu C, et al. Aberrant DNA methylation of P16, MGMT, and hMLH1 genes in combination with MTHFR C677T genetic polymorphism in esophageal squamous cell carcinoma. *Cancer Epidemiol Biomarkers Prev.* 2008;17:118–25.
20. Rice TW, Blackstone EH, Rusch VW. 7th edition of the *AJCC Cancer Staging Manual:* esophagus and esophagogastric junction. *Ann Surg Oncol.* 2010;17:1721–4.
21. Ogino S, Brahmandam M, Cantor M, et al. Distinct molecular features of colorectal carcinoma with signet ring cell component and colorectal carcinoma with mucinous component. *Mod Pathol.* 2006;19:59–68.
22. Ogino S, Kawasaki T, Brahmandam M, et al. Precision and performance characteristics of bisulfite conversion and real-time PCR (MethyLight) for quantitative DNA methylation analysis. *J Mol Diagn.* 2006;8:209–17.
23. Yang AS, Estecio MR, Doshi K, Kondo Y, Tajara EH, Issa JP. A simple method for estimating global DNA methylation using bisulfite PCR of repetitive DNA elements. *Nucleic Acids Res.* 2004;32:e38.
24. Estecio MR, Gharibyan V, Shen L, et al. LINE-1 hypomethylation in cancer is highly variable and inversely correlated with microsatellite instability. *PLoS One.* 2007;2:e399.
25. Ogino S, Kawasaki T, Nosho K, et al. LINE-1 hypomethylation is inversely associated with microsatellite instability and CpG island methylator phenotype in colorectal cancer. *Int J Cancer.* 2008;122:2767–73.
26. Irahara N, Nosho K, Baba Y, et al. Precision of pyrosequencing assay to measure LINE-1 methylation in colon cancer, normal colonic mucosa, and peripheral blood cells. *J Mol Diagn.* 2010; 12:177–83.
27. Baba Y, Huttenhower C, Nosho K, et al. Epigenomic diversity of colorectal cancer indicated by LINE-1 methylation in a database of 869 tumors. *Mol Cancer.* 2010;9:125.
28. Kawakami K, Matsunoki A, Kaneko M, Saito K, Watanabe G, Minamoto T. Long interspersed nuclear element-1 hypomethylation is a potential biomarker for the prediction of response to oral fluoropyrimidines in microsatellite stable and CpG island methylator phenotype-negative colorectal cancer. *Cancer Sci.* 2011;102:166–74.
29. Aparicio A, North B, Barske L, et al. LINE-1 methylation in plasma DNA as a biomarker of activity of DNA methylation inhibitors in patients with solid tumors. *Epigenetics.* 2009;4: 176–84.
30. Fakhrai-Rad H, Pourmand N, Ronaghi M. Pyrosequencing: an accurate detection platform for single nucleotide polymorphisms. *Hum Mutat.* 2002;19:479–85.
31. Ronaghi M. Pyrosequencing sheds light on DNA sequencing. *Genome Res.* 2001;11:3–11.
32. Ogino S, Chan AT, Fuchs CS, Giovannucci E. Molecular pathological epidemiology of colorectal neoplasia: an emerging transdisciplinary and interdisciplinary field. *Gut.* 2011;60: 397–411.
33. Schernhammer ES, Giovannucci E, Kawasaki T, Rosner B, Fuchs CS, Ogino S. Dietary folate, alcohol and B vitamins in relation to LINE-1 hypomethylation in colon cancer. *Gut.* 2010;59:794–9.
34. Sepulveda AR, Jones D, Ogino S, et al. CpG methylation analysis—current status of clinical assays and potential applications in molecular diagnostics: a report of the Association for Molecular Pathology. *J Mol Diagn.* 2009;11:266–78.
35. Speek M. Antisense promoter of human L1 retrotransposon drives transcription of adjacent cellular genes. *Mol Cell Biol.* 2001;21:1973–85.
36. Peaston AE, Evsikov AV, Graber JH, et al. Retrotransposons regulate host genes in mouse oocytes and preimplantation embryos. *Dev Cell.* 2004;7:597–606.
37. Faulkner GJ, Kimura Y, Daub CO, et al. The regulated retrotransposon transcriptome of mammalian cells. *Nat Genet.* 2009;41:563–71.
38. Han JS, Szak ST, Boeke JD. Transcriptional disruption by the L1 retrotransposon and implications for mammalian transcriptomes. *Nature.* 2004;429:268–74.
39. Yamada Y, Jackson-Grusby L, Linhart H, et al. Opposing effects of DNA hypomethylation on intestinal and liver carcinogenesis. *Proc Natl Acad Sci USA.* 2005;102:13580–5.
40. Howard G, Eiges R, Gaudet F, Jaenisch R, Eden A. Activation and transposition of endogenous retroviral elements in hypomethylation induced tumors in mice. *Oncogene.* 2008;27:404–8.
41. Chalitchagorn K, Shuangshoti S, Hourpai N, et al. Distinctive pattern of LINE-1 methylation level in normal tissues and the association with carcinogenesis. *Oncogene.* 2004;23:8841–6.

Ann Surg Oncol
DOI 10.1245/s10434-011-2068-6

Annals of
SURGICAL ONCOLOGY
OFFICIAL JOURNAL OF THE SOCIETY OF SURGICAL ONCOLOGY

ORIGINAL ARTICLE – TRANSLATIONAL RESEARCH AND BIOMARKERS

Carcinogenesis of Intraductal Papillary Mucinous Neoplasm of the Pancreas: Loss of MicroRNA-101 Promotes Overexpression of Histone Methyltransferase EZH2

Osamu Nakahara, MD[1], Hiroshi Takamori, MD[1], Masaaki Iwatsuki, MD[1], Yoshifumi Baba, MD[1], Yasuo Sakamoto, MD[1], Hiroshi Tanaka, MD[1], Akira Chikamoto, MD[1], Kei Horino, MD[1], Toru Beppu, MD[1], Keiichiro Kanemitsu, MD[3], Yumi Honda, MD[2], Ken-ichi Iyama, MD[2], and Hideo Baba, MD[1]

[1]Department of Gastroenterological Surgery, Graduate School of Medical Sciences, Kumamoto University, Kumamoto, Japan; [2]Department of Surgical Pathology, Graduate School of Medical Sciences, Kumamoto University, Kumamoto, Japan; [3]Department of Surgery, Saiseikai Kumamoto Hospital, Kumamoto, Japan

ABSTRACT

Background. The mechanisms of IPMN carcinogenesis are as yet unclear. This study aimed to determine whether expression of EZH2 promotes neoplastic progression of IPMN and PDCA, and to elucidate regulation of EZH2 expression by miR-101.

Methods. EZH2 mRNA and protein expression were investigated in 8 human pancreatic cancer cell lines by PCR and western blotting. Pre-miR-101 and anti-miR-101 were transfected into pancreatic cancer cells to elucidate EZH2 regulation by miR-101. To evaluate whether EZH2 modulates malignant progression of IPMN, EZH2 expression in IPMN was examined by immunohistochemistry. Next, we collected malignant and benign cells from FFPE samples of IPMNs using laser capture microdissection and extracted the RNA. miR-101 expression in IPMN was assessed using real-time PCR.

Results. All pancreatic cancer cell lines expressed EZH2 mRNA and protein. The induction of miR-101 by transfection of pre-miR-101 in MIA PaCa-2 was closely related to a reduction in EZH2 protein production compared with control, whereas there was little difference in the expression of EZH2 mRNA. Anti-miR-101 transfected pancreatic cancer cells showed an increase in EZH2 protein, while the level of EZH2 mRNA was not elevated. Immunohistochemistry revealed that the expression of EZH2 was significantly higher in malignant than benign IPMN. Expression of miR-101 was significantly lower in malignant IPMN than benign IPMN.

Conclusions. MiR-101 targets EZH2 at the posttranscriptional level, and loss of miR-101 could be a trigger for the adenomacarcinoma sequence of IPMN by upregulation of EZH2. This study suggests miR-101–EZH2 blockade as a potential therapeutic target in IPMN carcinogenesis.

Pancreatic ductal adenocarcinoma (PDCA) remains a lethal disease, with a fatality rate of 91%.[1] Approximately 230,000 patients per year develop PDCA worldwide and the overall 5-year survival rate ranges from 0.4 to 5%.[2–4] Improvements in survival rates remain limited despite recent advances in imaging technology and more effective treatments. A full understanding of the molecular mechanisms of carcinogenesis in PDCA is required to establish appropriate treatments and to improve the prognosis of PDCA. There were 3 precursors to PDCA proposed: pancreatic intraepithelial neoplasia (PanIN), mucinous cystic neoplasm (MCN), and intraductal papillary mucinous neoplasm (IPMN)[5]

Intraductal papillary mucinous neoplasm of the pancreas, denoting a pancreatic cystic lesion, was introduced into the World Health Organization (WHO) classification system in 1996 and since then has been increasingly reported worldwide.[6] Specifically, IPMN is an intraductal

Electronic supplementary material The online version of this article (doi:10.1245/s10434-011-2068-6) contains supplementary material, which is available to authorized users.

First Received: 7 March 2011

H. Baba, MD
e-mail: hdobaba@kumamoto-u.ac.jp

Published online: 20 September 2011

mucin-producing epithelial neoplasm that arises from a pancreatic duct, and WHO has established a histological classification for IPMN based on the degree of dysplasia: IPMN adenoma, IPMN borderline, and carcinoma. An adenomacarcinoma sequence has been proposed, and malignant alteration of IPMN has been investigated from various aspects such as oncogenes, tumor suppressor genes, cell cycle, and mucin production.[7–13] However, the mechanism of carcinogenesis is not yet fully understood.

MicroRNAs (miRNA) are approximately 22 nucleotide noncoding RNA molecules that usually operate as endogenous repressors of target genes. In animals, miRNAs can bind with imperfect complement to the 3′ untranslated region (3′ UTR) of the target mRNA via the RNA-induced silencing complex. Repression of the resulting gene occurs by multiple mechanisms including enhanced mRNA degradation and translational repression.[14] Developmental timing, cell death, proliferation, hematopoiesis, insulin secretion, and immune response are just a few examples of critical biological events that depend on accurate miRNA expression.[15] Many studies have shown that disturbances of miRNAs expression levels may have detrimental effects on cell physiology and may be directly implicated in the carcinogenic process.[16–20] These miRNAs, whose mutations or misexpressions correlate with various human neoplasms, are defined as "oncomiRs," and they can function as tumor suppressors or oncogenes.[21,22] Recently, the loss of miR-101 in prostrate cancer was reported to result in overexpression of enhancer of zeste 2 homolog (EZH2) and concomitant dysregulation of epigenetic pathways, leading to cancer progression.[23] The involvement of miR-101 in carcinogenesis through the regulation of EZH2 has been also demonstrated in bladder cancer, prostate cancer, lung cancer, gastric cancer, and glioblastoma.[23–28]

EZH2 gene encodes a polycomb group (PcG) protein, which acts as a histone methyltransferase and directly controls DNA methylation.[29–32] EZH2 is involved in several key regulatory mechanisms within eukaryotic cells, including control of embryonic development and cell proliferation.[33,34] Accumulating evidence has indicated an oncogenic role for EZH2 and its association with advanced pathologic features and the metastatic nature of cancer cells.[35–41] EZH2 may play an oncogenic role by down-regulating tumor suppressor genes.[38,42]

The natural history of IPMN and its progression to PDCA are not well defined. Moreover, little is known about any association between the carcinogenesis of IPMN and EZH2. Therefore, the aim of this study was to determine whether miR-101 regulates the expression of EZH2 during neoplastic progression from benign to malignant IPMN, and PDCA.

MATERIALS AND METHODS

Tissue Samples, Cell Lines, and Reagents

Formalin-fixed, paraffin-embedded (FFPE) tissues from 70 IPMN lesions (51 benign IPMN lesions and 19 malignant IPMN lesions) were used. The samples were obtained from a total of 54 patients who underwent pancreatic resection of either benign, malignant, or both benign and malignant lesions at some time between 1997 and 2009 at Department of Gastroenterological Surgery, Kumamoto University. All patients provided written informed consent for the use of their tissues. The characteristics of these patients are shown in Table 1. The experimental protocol was approved by the institutional review board of Kumamoto University.

There were seven pancreatic cancer cell lines (PANC-1, PK8, PK9, PK-59, KLM-1, MIA Paca2, PK-45P) obtained from the Cell Resource Center for Biomedical Research Institute of Development, Aging, and Cancer, Tohoku University, Japan. Hs-700T was purchased from the American Type Cell Culture (Rockville, MD). The cells were cultured in RPMI 1640 medium (Invitrogen, Carlsbad, CA) supplemented with 10% fetal bovine serum at 37°C under 5% CO_2 and 95% air humidity atmosphere.

Immunohistochemical Procedures and Evaluation of EZH2 Expression Immunohistochemical staining was performed on 3-μm sections obtained from FFPE blocks. Endogenous peroxidase activity was blocked using 3% hydrogen peroxide for 5 minutes. The sections were

TABLE 1 Characteristics of 54 patients with IPMNs

Characteristic		No. of IPMCa lesions (%)
Age (years)		
Mean	69.1	
Range	48–81	
Sex		
Male	38	
Female	16	
Type of IPMN		
Main duct	19	15 (79%)
Branch duct	35	4 (11%)
Morphological subtype		
Gastric	38	7 (18%)
Intestinal	8	5 (63%)
Pancreatobiliary	3	2 (67%)
Oncocytic	3	3 (100%)
Unclassified	2	2 (100%)

incubated in 50× diluted primary mouse monoclonal anti-EZH2 antibodies (BD Transduction Laboratories) overnight at 4°C. A subsequent reaction was performed with a biotin-free horseradish peroxidase enzyme-labeled polymer of the Envision Plus detection system (Dako Co., Tokyo, Japan). A positive reaction was visualized with a diaminobenzidine solution, followed by counterstaining with Mayer's hematoxylin. Two pathologists were blinded to any information on samples and elevations in the expression of EZH2. The number of EZH2-positive cells of the total number of IPMN cells was counted in 5-high power field (HPF), and positive rates were calculated.

Microdissection-Based Quantitative Analysis of miR-101 Paired malignant and benign samples were collected from the same FFPE tissues in five IPMN cases by means of laser microdissection. Researchers placed 7-μm thick FFPE sections on Director laser microdissection slides (Expression Pathology, Gaithersburg, MD), deparaffinized, and stained with hematoxylin and eosin (H&E). Parts of the sections 3 mm^2 in area were then microdissected using a laser microdissection and pressure catapulting system (P.A.L.M. Microlaser Technologies, Bernried, Germany). Total RNA was extracted from the selected cells using RecoverAll Total Nucleic Acid Isolation Kit for FFPE (Cat. No. 1975; Ambion, Austin, TX) according to the manufacturer's instructions and subjected to real-time RT-PCR for quantitative measurement of miR-101. The quality of RNA was determined by a NanoDrop 2000c (Thermo Fisher Scientific, Wilmington, DE). For quality control, samples with insufficient tumor tissue, insufficient RNA, or a weak RT-PCR signal (average cycle threshold for the reference genes: >35) were excluded.

Real-Time PCR-Based Detection of microRNA-101 and EZH2 mRNA Total RNA was obtained from cell lines using the mirVana microRNA isolation kit (Ambion), according to the manufacturer's instructions. The expression of mature microRNAs was determined by TaqMan quantitative real-time PCR using the TaqMan microRNA assay (Applied Biosystems) and normalized using the $2^{-\Delta\Delta}$ CT method relative to U6-small nuclear RNA. EZH2 mRNA was quantified by SYBR-Green quantitative real-time PCR and normalized to glyceraldehyde-3-phosphate dehydrogenase.[4,3] PCR primers were as follows: EZH2, 5′-tttcca gataagggcacagc-3′ (forward) and 5′-cgcctacagaaaagcgta tg-3′ (reverse), and glyceraldehyde-3-phosphate dehydrogenase, 5′-tgaccacagtccatgccatc-3′ (forward) and 5-ccaccc tgttgctgtagcc-3′ (reverse). All PCR procedures were performed in triplicate.

Western Blotting To isolate the proteins, cells harvested in 6-well plates were washed once in phosphate-buffered saline (PBS) and lysed in the lysis buffer [Tris–HCl (pH 7.4), 25 mmol/l; NaCl, 100 mmol/l; EDTA, 2 mmol/l; Triton X, 1%; with 10 μg/ml aprotinin, 10 μg/ml leupeptin, 1 mmol/l Na_3VO_4, 1 mmol/l phenylmethylsulfonylfluoride]. SDS-PAGE and western blotting were performed according to standard procedures. Western blotting of β-actin on the same membrane was used as a loading control. The signals were detected by secondary antibodies labeled with ECL Detection System (GE Healthcare).

Forced Expression and Knockdown of miR-101 To examine the effect of miR-101 overexpression, pre-miR-101 or pre-miR-Scramble was transfected into MIA PaCa2 cells. Similarly, to examine the effect of miR-101 knockdown, the Anti-miR miRNA Inhibitor (Ambion) or the Anti-miR miRNA Inhibitors-Negative Control was transfected into PK-8 cells. The cells were seeded at a density of 1.0×10^5 cells in 6-well tissue culture plates for 24 h, followed by transfection with 50 nM of all miR transfectants. These cells were subjected to protein and RNA extraction.

Statistical Analysis Statistical analysis was performed using the StatView 5.0 software program (SAS Institute). Values are expressed as the mean ± SD. Differences/correlations between groups were calculated with *t* test, the Mann–Whitney *U* test, and Pearson's correlation test. Statistical significance was defined as $P < 0.05$.

RESULTS

All Pancreatic Cancer Cell Lines Expressed EZH2 mRNA and Protein

We used RT-PCR and western blotting to assess the expression of EZH2 in eight human pancreatic cancer cell lines. All pancreatic cancer cell lines expressed similar levels of EZH2 mRNA (Fig. 1a). The levels of EZH2 protein in these cells were not markedly different from each other overall, even though some cell lines showed a moderate degree of inverse correlation between the miR-101 (Fig. 1c) and EZH2 (Fig. 1b) protein levels compared with the levels of β-actin.

Overexpression of miR-101 Decreased EZH2 Protein We assessed the effect of the overexpression of miR-101 on EZH2 protein. Pre-miR-101 transfected MIA PaCa2 cells revealed a significant increase in miR-101 expression compared with the negative control, measured by qRT-PCR (Fig. 2a). Western blot analysis of EZH2 in MIAPaCa2 cells showed that miR-101 overexpression reduced EZH2 protein production compared with Scr

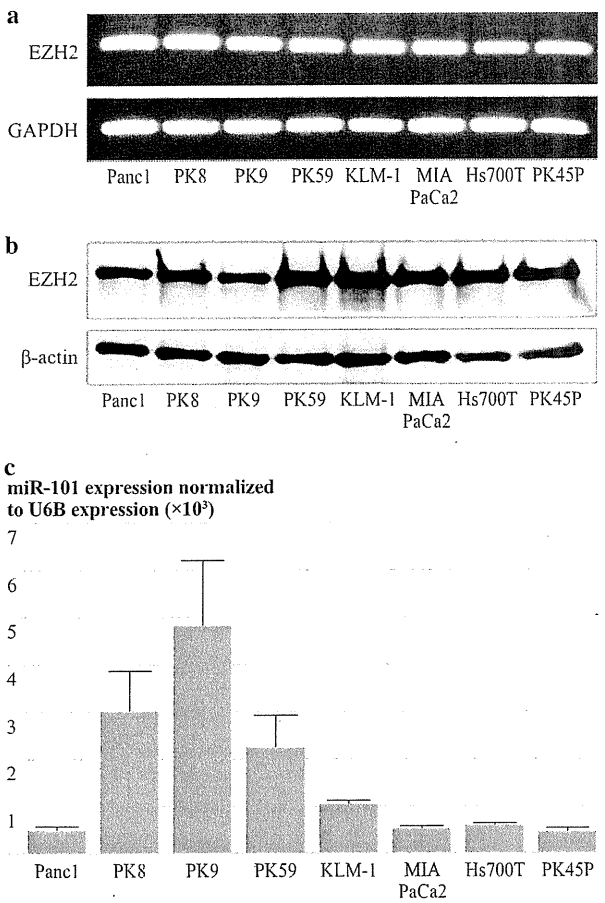

FIG. 1 **a** Expression of EZH2 mRNA in pancreatic cancer cell lines as determined by RT-PCR. **b** Expression of EZH2 protein in pancreatic cancer cell lines as determined by western blotting. Data normalized against GAPDH mRNA and β-actin protein expression. **c** MicroRNA-101 in pancreatic cancer cell lines as determined by real-time PCR. Data normalized against expression of U6B RNA

transfected cells (Fig. 2c), whereas quantitative real-time PCR revealed little difference in the EZH2 mRNA level between cells overexpressing miR-101 and controls (Fig. 2b). Furthermore, the proliferation of MIA PaCa2 cells transfected with pre-miR-101 was significantly suppressed compared with the control (Supplement Fig. 1).

Decreased Expression of miR-101 Increased EZH2 Protein The effect of miR-101 transfection on EZH2 protein expression was evaluated in PK-8 cells, which possess the second highest level of endogenous miR-101 among the eight pancreatic cancer cell lines (Fig. 1c). Anti-miR-101 transfected cells showed decreased miR-101 levels and an increase in EZH2 protein (Fig. 2d, f), whereas the level of EZH2 mRNA was not elevated (Fig. 2e).

Expression of EZH2 in IPMN Expression of EZH2 was examined in a total of 51 lesions of benign IPMN, four lesions of carcinoma in situ, and 15 lesions of invasive carcinoma derived from IPMN by IHC. EZH2 was observed in cell nuclei in both carcinoma in situ and in invasive parts of malignant IPMN, whereas benign IPMN showed little expression (Fig. 3a–c). Quantitative analyses of EZH2 revealed that the carcinoma in situ was 49% positive, ranging from 26 to 71%, and the invasive carcinoma was 50% positive, ranging from 0 to 95%, while expression of EZH2 was 5.4%, ranging from 0 to 50%, in benign lesions. These findings indicated that the expression of EZH2 was significantly higher, not only in carcinoma in situ, but also in the invasive parts, than in benign IPMN. There was, however, no statistical difference in expression of EZH2 between carcinoma in situ and the invasive parts (Fig. 3d).

MicroRNA-101 Expression Lower in Malignant than in Benign IPMN We measured expression of miR-101 in both malignant and benign IPMN cells by qRT-PCR after collection of cells by laser microdissection in five patients. First, we assessed the quality of RNA taken from FFPE tissues. All RNA (A260/A280) was indicated as between 1.10 and 2.70 to confirm suitability for RT-PCR. The expression of MiR-101 was significantly less in malignant IPMN than in benign IPMN ($P = 0.009$; Fig. 4).

DISCUSSION

All eight pancreatic cancer cell lines clearly expressed EZH2. EZH2 is a member of the Polycomb group (PcG) proteins, which regulate epigenetically mediated transcriptional silencing, are involved in the maintenance of embryonic and adult stem cells, and have been implicated in cancer development.[44] EZH2 is upregulated in several kinds of neoplasms, including leukemia, prostate cancer, and breast cancer.[37,38,45–47] Interestingly, high expression of EZH2 localizes to more malignant cell types and is associated with metastatic nature of cancer cells.[39–41,47,48] A previous report revealed that pancreatic cancer cell lines expressed EZH2, which contributed to cell proliferation.[49] We could confirm such expression in pancreatic cancers. Moreover, our results revealed that synthetic exogenous miR-101 induced significant silencing of EZH2 in pancreatic cancer cells, and anti-miR-101 transfected pancreatic cancer cells showed an increase in EZH2 protein at the posttranscriptional level. A corresponding loss of miR-101 in bladder cancer led to overexpression of EZH2.[23,24] This indicates that PDCAs express EZH2, caused by loss of miR-101.

We next investigated whether miR-101 can induce EZH2 silencing in the malignant transformation of IPMN.

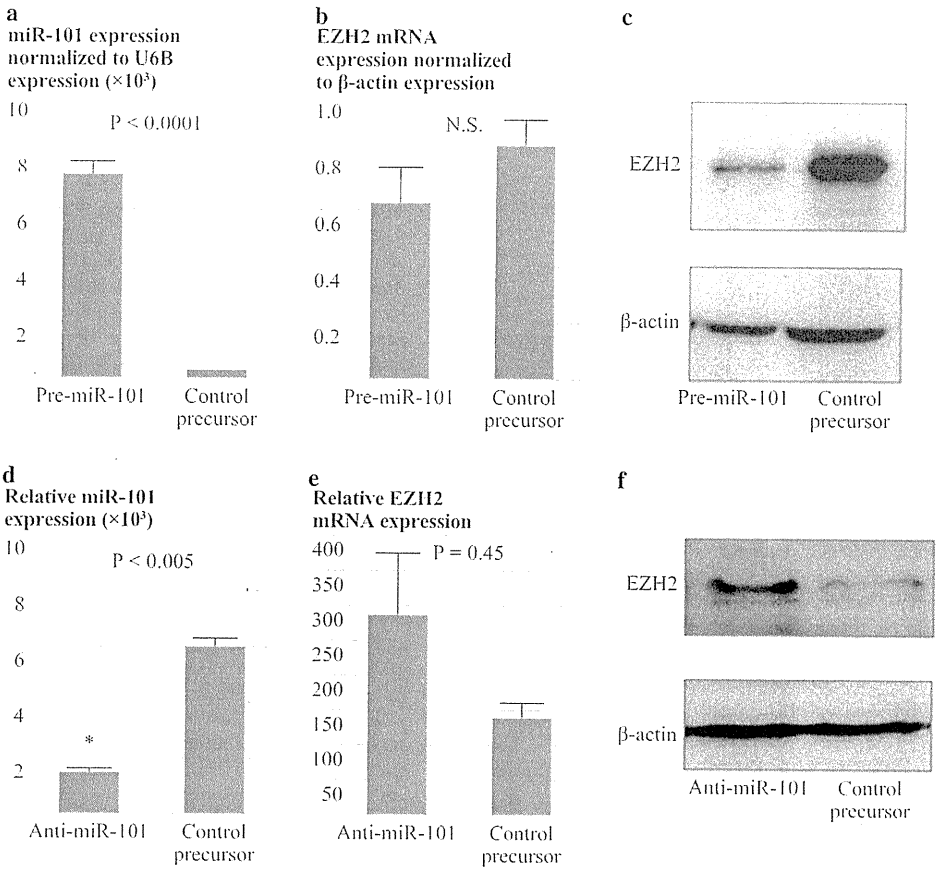

FIG. 2 Overexpression of microRNA-101 downregulates EZH2 expression at the posttranscriptional level. **a** MicroRNA-101 expression analyzed after transfection of pre-miR-101 by TaqMan-quantitative real-time PCR in MIA PaCa2 cells. Expression levels normalized to the expression of U6B, and presented as relative microRNA-101 expression. **b** EZH2 mRNA expression analyzed after transfection of pre-miR-101 by quantitative real-time PCR in MIA PaCa2 cells. Expression levels normalized to β-actin expression, and presented as relative EZH2 expression. **c** EZH2 protein expression analyzed by western blotting after transfection of pre-miR-101 in MIA PaCa2 cells. Membranes blotted by anti-EZH2 IgG and anti-β-actin IgG. **d** microRNA-101 expression analyzed by TaqMan-quantitative real-time PCR. Results are normalized to U6B expression and presented as relative microRNA-101 expression. $^*P < 0.05$. **e** EZH2 mRNA expression analyzed by quantitative real-time PCR. The results are normalized to β-actin expression and are presented as relative EZH2 expression. **f** Cells lysates were analyzed by western blotting. Membranes were blotted by anti-EZH2 IgG and anti-β-actin IgG

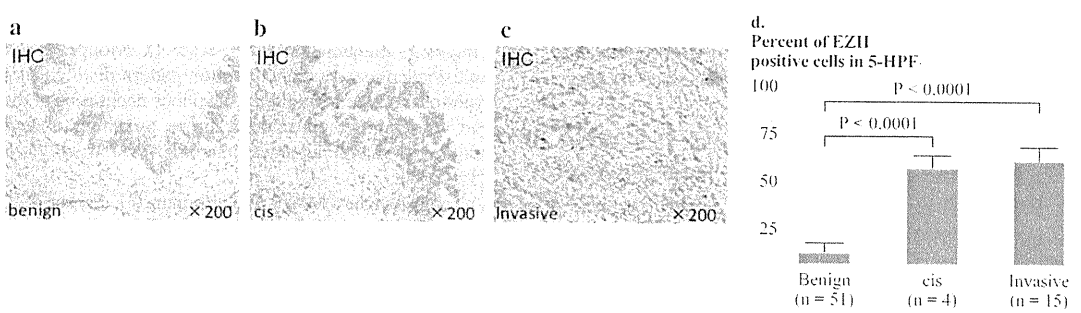

FIG. 3 Detection of EZH2 in IPMN tissues by immunohistochemistry. **a** IPMA showed no significant staining of EZH2. EZH2 was detected as strongly positive stains in not only carcinoma in situ (cis) **b** but also invasive carcinoma derived from IPMN (**c**). **d** Quantitative analyses of EZH2 expression in IPMA, cis, and invasive lesions by immunohistochemistry. Expression of EZH2 was significantly higher in cis and invasive parts compared with IPMA ($P < 0.0001$), but not between cis and invasive lesions

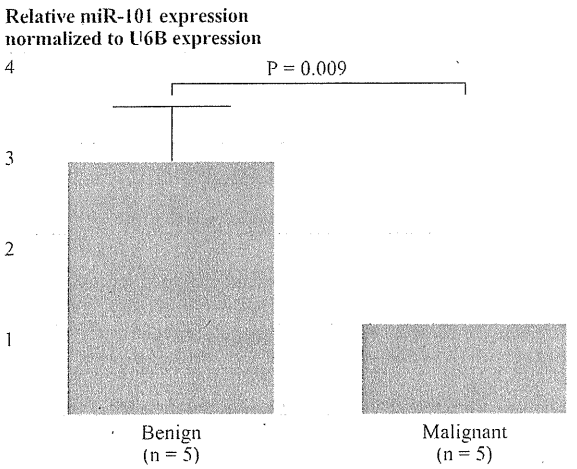

FIG. 4 Comparison of average level of miR-101 expression in five patients with both benign and malignant IPMN. MiR-101 levels analyzed by real-time PCR and data normalized against U6 RNA expression. Relative expression of each tumor sample refers to the normal sample of the same patient. miR-101 expression was significantly lower in malignant than benign IPMN ($P = 0.0001$)

Expression of EZH2 was significantly higher in malignant than benign IPMN. Moreover, expression of miR-101 was significantly decreased in malignant cells compared with benign cells of IPMN. These results indicated that miR-101 could downregulate EZH2 in benign IPMN, while a reduced level of miR-101 is attributable to increased expression of EZH2 in malignant IPMN. Habbe et al.[50] suggested that miR-155 might be a biomarker of early pancreatic neoplasia, but the mechanism of carcinogenesis of IPMN and miR-155 was not evaluated.

Genetic alterations that have been described in the transformation from benign to malignant IPMN include cyclooxygenase 2, p16, DPC4/Smad4, p53, K-ras, and apomucins.[11,12,51,52] However, unanswered questions remain. We could clarify that EZH2 expression was significantly higher in malignant than benign IPMN by means of immunohistochemical analysis. This indicated that overexpression of EZH2 could promote malignant transformation of IPMN. This regulation could be one of the mechanisms of IPMN carcinogenesis.

Based on these considerations, we conclude that miR-101 targets EZH2 at the posttranscriptional level and that loss of miR-101 could be a trigger for the adenomacarcinoma sequence of IPMN by upregulation of EZH2. This study suggests that miR-101 EZH2 blockade is a potential therapeutic target in IPMN carcinogenesis. Because recent studies reported an increase in the angiogenesis index of IPMN and an involvement of miR-101 in angiogenesis through EZH2 in endothelial cells, it would be of great interest to determine a role of EZH2 and miR-101 in the angiogenesis of IPMN.[28,53]

ACKNOWLEDGMENT We thank Hirohisa Okabe and Takihiro Kamio for their cooperation in this study.

REFERENCES

1. American Cancer Society. Cancer facts and figures 2008. Atlanta: American Cancer Society; 2008.
2. Parkin DM, Bray F, Ferlay J, Pisani P. Global cancer statistics, 2002. *CA Cancer J Clin.* 2005;55:74–108.
3. Bramhall SR, Allum WH, Jones AG, Allwood A, Cummins C, Neoptolemos JP. Treatment and survival in 13,560 patients with pancreatic cancer, and incidence of the disease, in the West Midlands: an epidemiological study. *Br J Surg.* 1995;82:111–5.
4. Jemal A, Siegel R, Ward E, Hao Y, Xu J, Murray T, et al. Cancer statistics, 2008. *CA Cancer J Clin.* 2008;58:71–96.
5. Hruban RH, Pitman MB, Klimstra DS. Tumors of the pancreas. In: Armed Forces Institute of Pathology, 4th ed. Washington, DC: The American Registry of Pathology; 2007. p. 75–164.
6. Klöppel GSE, Longnecker DS. Histological typing of tumours of the exocrine pancreas. In: World Health Organization International Histological Classification of Tumours, 2nd ed. Berlin: Springer; 1996. p. 12–9.
7. Sessa F, Solcia E, Capella C, Bonato M, Scarpa A, Zamboni G, et al. Intraductal papillary-mucinous tumours represent a distinct group of pancreatic neoplasms: an investigation of tumour cell differentiation and K-ras, p53 and c-erbB-2 abnormalities in 26 patients. *Virchows Arch.* 1994;425:357–67.
8. Nagai E, Ueki T, Chijiiwa K, Tanaka M, Tsuneyoshi M. Intraductal papillary mucinous neoplasms of the pancreas associated with so-called "mucinous ductal ectasia." Histochemical and immunohistochemical analysis of 29 cases. *Am J Surg Pathol.* 1995;19:576–89.
9. Tanaka M, Kobayashi K, Mizumoto K, Yamaguchi K. Clinical aspects of intraductal papillary mucinous neoplasm of the pancreas. *J Gastroenterol.* 2005;40:669–75.
10. Yoshizawa K, Nagai H, Sakurai S, Hironaka M, Morinaga S, Saitoh K, et al. Clonality and K-ras mutation analyses of epithelia in intraductal papillary mucinous tumor and mucinous cystic tumor of the pancreas. *Virchows Arch.* 2002;441:437–43.
11. Biankin AV, Biankin SA, Kench JG, Morey AL, Lee CS, Head DR, et al. Aberrant p16(INK4A) and DPC4/Smad4 expression in intraductal papillary mucinous tumours of the pancreas is associated with invasive ductal adenocarcinoma. *Gut.* 2002;50:861–8.
12. Niijima M, Yamaguchi T, Ishihara T, Hara T, Kato K, Kondo F, et al. Immunohistochemical analysis and in situ hybridization of cyclooxygenase-2 expression in intraductal papillary-mucinous tumors of the Pancreas. *Cancer.* 2002;94:1565–73.
13. Luttges J, Zamboni G, Longnecker D, Kloppel G. The immunohistochemical mucin expression pattern distinguishes different types of intraductal papillary mucinous neoplasms of the pancreas and determines their relationship to mucinous noncystic carcinoma and ductal adenocarcinoma. *Am J Surg Pathol.* 2001; 25:942–8.
14. Valencia-Sanchez MA, Liu J, Hannon GJ, Parker R. Control of translation and mRNA degradation by miRNAs and siRNAs. *Genes Dev.* 2006;20:515–24.
15. Ambros V. The functions of Animal microRNAs. *Nature.* 2004;431:350–5.
16. Chan JA, Krichevsky AM, Kosik KS. MicroRNA-21 is an antiapoptotic factor in human glioblastoma cells. *Cancer Res.* 2005;65:6029–33.
17. Iorio MV, Ferracin M, Liu CG, Veronese A, Spizzo R, Sabbioni S, et al. MicroRNA gene expression deregulation in human breast cancer. *Cancer Res.* 2005;65:7065–70.